

AD-A145 716

MOMENT INDUCED BY LIQUID PAYLOAD DURING SPIN-UP WITHOUT
A CRITICAL LAYER. (U) ARMY ARMAMENT RESEARCH AND
DEVELOPMENT CENTER ABERDEEN PROVIN. C H MURPHY AUG 84

1/1

UNCLASSIFIED

ARBRL-TR-02581 SBI-AD-F300 461

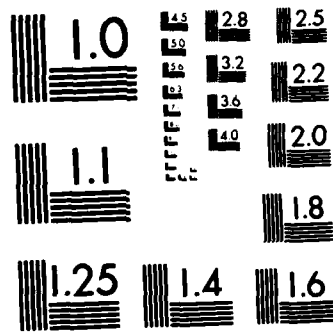
F/G 19/1

NL

END

FORM

DTIC



MICROCOPY RESOLUTION TEST CHART
NATIONAL BUREAU OF STANDARDS-1963-A

12

AD /

AD-A145 716

TECHNICAL REPORT ARBRL-TR-02581

MOMENT INDUCED BY LIQUID PAYLOAD
DURING SPIN-UP WITHOUT A
CRITICAL LAYER

Charles H. Murphy

August 1984



US ARMY ARMAMENT RESEARCH AND DEVELOPMENT CENTER
BALLISTIC RESEARCH LABORATORY
ABERDEEN PROVING GROUND, MARYLAND

Approved for public release; distribution unlimited.

DTIC FILE COPY

DTIC
ELECTE
SEP 13 1984
S E D

84 09 05 023

Destroy this report when it is no longer needed.
Do not return it to the originator.

Additional copies of this report may be obtained
from the National Technical Information Service,
U. S. Department of Commerce, Springfield, Virginia
22161.

The findings in this report are not to be construed as an official
Department of the Army position, unless so designated by other
authorized documents.

The use of trade names or manufacturers' names in this report
does not constitute indorsement of any commercial product.

UNCLASSIFIED

SECURITY CLASSIFICATION OF THIS PAGE (When Data Entered)

REPORT DOCUMENTATION PAGE		READ INSTRUCTIONS BEFORE COMPLETING FORM
1. REPORT NUMBER TECHNICAL REPORT ARBRL-TR-02581	2. GOVT ACCESSION NO. ADA145716	3. RECIPIENT'S CATALOG NUMBER
4. TITLE (and Subtitle) MOMENT INDUCED BY LIQUID PAYLOAD DURING SPIN-UP WITHOUT A CRITICAL LAYER	5. TYPE OF REPORT & PERIOD COVERED Final	
	6. PERFORMING ORG. REPORT NUMBER	
7. AUTHOR(s) CHARLES H. MURPHY	8. CONTRACT OR GRANT NUMBER(s)	
9. PERFORMING ORGANIZATION NAME AND ADDRESS US Army Ballistic Research Laboratory ATTN: DRXBR-LFD Aberdeen Proving Ground, Maryland 21005-5066	10. PROGRAM ELEMENT, PROJECT, TASK AREA & WORK UNIT NUMBERS RDT&E 1L161102AH43	
11. CONTROLLING OFFICE NAME AND ADDRESS US Army Ballistic Research Laboratory ATTN: DRXBR-OD-ST Aberdeen Proving Ground, Maryland 21005-5066	12. REPORT DATE August 1984	
	13. NUMBER OF PAGES 55	
14. MONITORING AGENCY NAME & ADDRESS (if different from Controlling Office)	15. SECURITY CLASS. (of this report) UNCLASSIFIED	
	15a. DECLASSIFICATION/DOWNGRADING SCHEDULE	
16. DISTRIBUTION STATEMENT (of this Report) Approved for public release; distribution unlimited.		
17. DISTRIBUTION STATEMENT (of the abstract entered in Block 20, if different from Report)		
18. SUPPLEMENTARY NOTES This report supersedes IMR 774, dated April 1983.		
19. KEY WORDS (Continue on reverse side if necessary and identify by block number) Critical Layer Liquid-Filled Shell Spin-Up Stability		
20. ABSTRACT (Continue on reverse side if necessary and identify by block number) (bja) For a fully spun-up liquid payload, eigenfrequencies and liquid side moments induced by projectile coning motion have been computed by a linear boundary layer theory. For partially spun-up liquids, this theory can fail due to the presence of a critical layer in which the local angular velocity of the spinning motion is near the angular velocity of the projectile's coning motion. (continued)		

UNCLASSIFIED

SECURITY CLASSIFICATION OF THIS PAGE(When Data Entered)

Late in the spin-up process, when more than 90% of the spin angular momentum has been acquired by the liquid, a critical layer usually does not exist. In this report, a linear-boundary-layer theory is developed to predict eigenfrequencies and the liquid moment during late spin-up times. The predicted eigenfrequencies agree well with those computed by the linearized Navier-Stokes technique of Gerber and Sedney. The side moments predicted by the linear-boundary-layer theory are available to projectile designers for flight stability analysis.

UNCLASSIFIED

SECURITY CLASSIFICATION OF THIS PAGE(When Data Entered)

TABLE OF CONTENTS

	<u>Page</u>
LIST OF ILLUSTRATIONS.....	5
I. INTRODUCTION.....	7
II. BASIC EQUATIONS.....	9
III. EIGENVALUES.....	17
IV. STEADY-STATE SOLUTION.....	18
V. LIQUID MOMENT.....	23
VI. NUMERICAL CALCULATIONS.....	24
Table 1. Comparison of Navier-Stokes and Linear-Boundary- Layer Eigenvalues for $m = 0$, $k = 2$, $c/a = .995$, $\kappa = .500$	25
Table 2. Comparison of Navier-Stokes and Linear-Boundary- Layer Eigenvalues for $m = 1$, $k = 1$, $c/a = .600$, $\kappa = .443$	25
VII. SUMMARY.....	26
ACKNOWLEDGMENT.....	27
REFERENCES.....	37
APPENDIX A.....	39
LIST OF SYMBOLS.....	43
DISTRIBUTION LIST.....	49

Accession For	
NTIS GRA&I	<input checked="" type="checkbox"/>
DTIC TAB	<input type="checkbox"/>
Unannounced	<input type="checkbox"/>
Justification	
By _____	
Distribution/	
Availability Codes	
Dist	Avail and/or Special
A-1	



LIST OF ILLUSTRATIONS

<u>Figure</u>		<u>Page</u>
1	Laminar Flow Solutions of Eq. (2.5) for $Re = 40,000$, $c/a = 4$, $\phi = 800$ rad.....	28
2	Laminar Flow Solutions of Eq. (2.5) for $Re = 40,000$, $c/a = 4$, $\phi = 2600$ rad.....	29
3	Liquid Angular Momentum Ratio vs ϕ/\sqrt{Re} for $c/a = 4$	30
4	Spin Angles for which $\hat{w}_0 = 0.11$ vs Reynolds number, $c/a = 4$	31
5	Eigenfrequency τ_{31} vs Spin Angle ϕ for $Re = 40,000$, $c/a = 3.12$, $k = 3$, $n = 1$, $\kappa = 0.443$. The Curves are from Sedney-Gerber NS Theory (Fig. 5, Ref. 16), the Circles are from Linear-Boundary-Layer Theory.....	32
6	Eigenfrequency τ_{3n} vs Spin Angle ϕ for $Re = 5000$, $c/a = 3.297$, $k = 3$, $\kappa = 0.443$. The Curves are from Sedney-Gerber NS Theory (Fig. 6, Ref. 16), the Circles are from Linear-Boundary-Layer Theory.....	33
7	Liquid Side Moment Coefficient C_{LSM} vs Spin Angle for $\tau = .08$ and the Conditions of Figure 5.....	34
8	Ratio of Maximum Side Moment Coefficients vs Roll Angle, ϕ for $Re = 4 \times 10^4$, 2×10^6 , $c/a = 3.12$, $k = 3$, $n = 1$	35
9	Ratio of Maximum Side Moment Coefficients vs Roll Angle, for $Re = 4974$, $c/a = 3.297$, $k = 3$, $n = 1,2$	36

I. INTRODUCTION

The prediction of the complete moment exerted by a spinning liquid payload on a spinning and coning projectile has been a problem of considerable interest to the Army for some time. For a fully spinning liquid, the linear side moment was first computed by Stewartson¹ for an inviscid payload by use of eigenfrequencies determined by the fineness ratio of the cylindrical container. Wedemeyer² introduced boundary layers on the walls of the container and was able to determine viscous corrections for Stewartson's eigenfrequencies, which could then be used in Stewartson's side moment calculation. Murphy³ then completed the linear boundary layer theory by including all pressure and wall shear contributions to the liquid-induced side moment. The Stewartson-Wedemeyer eigenvalue calculations have been improved for low Reynolds numbers by Kitchens et al.⁴ through the replacement of the cylindrical wall boundary approximation by a linearized Navier-Stokes approach. Next Gerber et al.⁵⁻⁶ extended this linearized NS technique to compute better side moment coefficients for Reynolds numbers less than 10,000. Finally, the roll moment for a fully spun-up liquid was computed by Murphy.⁷

Since liquid payloads can require as much as half the flight time to reach full spin-up,⁸ considerable theoretical effort has been expended on

1. K. Stewartson, "On the Stability of a Spinning Top Containing Liquid," *Journal of Fluid Mechanics*, Vol. 5, Part 4, September 1959, pp. 577-592.
2. E.H. Wedemeyer, "Viscous Correction to Stewartson's Stability Criterion," *Ballistic Research Laboratory, Aberdeen Proving Ground, Maryland, BRL Report 1325, June 1966. (AD 489687)*
3. C.H. Murphy, "Angular Motion of a Spinning Projectile With a Viscous Liquid Payload," *Ballistic Research Laboratory, Aberdeen Proving Ground, Maryland, BRL Memorandum Report ARBRL-MR-03194, August 1982. (AD A118676) (See also Journal of Guidance, Control, and Dynamics, Vol. 6, July-August 1983, pp. 280-286.)*
4. C.W. Kitchens, Jr., N. Gerber, and R. Sedney, "Oscillations of a Liquid in a Rotating Cylinder: Solid Body Rotation," *Ballistic Research Laboratory, Aberdeen Proving Ground, Maryland, BRL Technical Report BRL-TR-02081, June 1978. (AD A057759)*
5. N. Gerber, R. Sedney, and J.M. Bartos, "Pressure Moment on a Liquid-Filled Projectile: Solid Body Rotation," *Ballistic Research Laboratory, Aberdeen Proving Ground, Maryland, BRL Technical Report ARBRL-TR-02422, October 1982. (AD A120567)*
6. N. Gerber and R. Sedney, "Moment on a Liquid-Filled Spinning and Nutating Projectile: Solid Body Rotation," *Ballistic Research Laboratory, Aberdeen Proving Ground, Maryland, BRL Technical Report ARBRL-TR-02470, February 1983. (AD A125332)*
7. C.H. Murphy, "Liquid Payload Roll Moment Induced by a Spinning and Coning Projectile," *Ballistic Research Laboratory, Aberdeen Proving Ground, Maryland, BRL Technical Report ARBRL-TR-02521, September 1983. (AD A133681) (See also AIAA Paper 83-2142, August 1983.)*
8. A. Mark, "Measurements of Angular Momentum Transfer in Liquid-Filled Projectiles," *Ballistic Research Laboratory, Aberdeen Proving Ground, Maryland, BRL Technical Report BRL-TR-02029, November 1977. (AD A051056)*

predicting the spin-up process and its effect on the liquid-induced moment. Wedemeyer⁹ developed a very simple model of the spin-up process, which was extended by other authors.¹⁰⁻¹² The calculation of eigenvalues and side moment during spin-up is, however, a difficult task. Karpov¹³ made use of a Wedemeyer suggestion to obtain an approximation for the liquid side moment. Reddi¹⁴ attempted to solve the inviscid perturbation equations but had considerable difficulty with a singular critical layer which is usually present. A critique of this work is given by Lynn¹⁵ who did get a solution for axisymmetric waves for which no critical layer is present. Sedney and Gerber¹⁶ extended their linearized Navier-Stokes perturbation to calculate spin-up eigenfrequencies in the presence of a critical layer.

Although Sedney and Gerber have been able to overcome the mathematical difficulties associated with the singular critical layer, their method requires the solution of six complicated first order differential equations. This critical layer occurs in an annular region in which the angular velocity of the liquid spinning motion is near the angular frequency of the projectile's coning motion. Fortunately, late in the spin-up process the critical layer does not usually exist, and the simple linear boundary layer theory can be successfully extended to predict late spin-up eigenfrequencies and liquid side moment. As we shall see, this approach involves the solution of only one second order differential equation.

-
9. E.H. Wedemeyer, "The Unsteady Flow Within a Spinning Cylinder," *Journal of Fluid Mechanics*, Vol. 20, Part 3, 1964, pp. 383-399. (See also BRL Report 1225, October 1963, (AD 431846).)
 10. C.W. Kitchens, Jr., "Ekman Compatibility Conditions in Wedemeyer Spin-Up Model," *Physics of Fluids*, Vol. 23, Part 5, May 1980, pp. 1062-1064.
 11. C.W. Kitchens, Jr., N. Gerber, and R. Sedney, "Spin Decay of Liquid-Filled Projectiles," *Journal of Spacecraft and Rockets*, Vol. 15, November-December 1978, pp. 348-354. (See also BRL Report 1996, July 1977, (AD A043275), and BRL Report 2026, October 1977, (AD A050311).)
 12. R. Sedney and N. Gerber, "Viscous Effects in the Wedemeyer Model of Spin-Up From Rest," *Ballistic Research Laboratory, Aberdeen Proving Ground, Maryland, BRL Technical Report ARBRL-TR-02493, June 1983. (AD A129506)*
 13. B.G. Karpov, "Dynamics of Liquid-Filled Shell: Instability During Spin-Up," *Ballistic Research Laboratory, Aberdeen Proving Ground, Maryland, BRL Memorandum Report BRL-MR-1629, January 1965. (AD 463926)*
 14. M.M. Reddi, "On the Eigenvalues of Couette Flow in a Fully-Filled Cylindrical Container," *Franklin Institute Research Laboratory, Philadelphia, PA, Report No. F-B2294, 1967.*
 15. Y.M. Lynn, "Free Oscillations of a Liquid During Spin-Up," *Ballistic Research Laboratory, Aberdeen Proving Ground, Maryland, BRL Report No. 1663, August 1973. (AD 769710)*
 16. R. Sedney and N. Gerber, "Oscillations of a Liquid in a Rotating Cylinder Part II. Spin-Up," *Ballistic Research Laboratory, Aberdeen Proving Ground Maryland, BRL Technical Report ARBRL-TR-02489, May 1983. (AD A129094)*

In this report we will derive this theory for a liquid near full spin-up and determine validity bounds in terms of flight time. Eigenfrequencies computed by this basically inviscid theory are shown to compare very well with those computed by the Gerber-Sedney linearized Navier-Stokes theory. Finally, side moment calculations are made to show the significant changes that occur during this late spin-up period.

II. BASIC EQUATIONS

We will consider a fully-filled cylindrical cavity with radius, a , and height, $2c$. According to Wedemeyer,⁹ the spin-up flow is driven by Ekman layer flows at the flat end walls. These Ekman layers draw fluid in near the axis, impart rotation to it, and eject it near the cylindrical wall. The flow exterior to these Ekman layers on the end walls and a boundary layer (Stewartson layer)¹² on the cylindrical lateral walls can be approximated by a two-dimensional rotating flow with circumferential velocity V_θ . A projectile attains full spin during 10-20 milli-seconds of motion down a gun barrel. If the spin is assumed to grow from an impulsive start at zero spin to a constant value of $\dot{\phi}$, the resulting circumferential velocity has the form

$$V_\theta = r \dot{\phi} \hat{w}(r, \phi) \quad (2.1)$$

where $\phi = \dot{\phi}t$. The boundary conditions for \hat{w} are*

$$\hat{w}(r, 0) = 0 \quad 0 \leq r < a \quad (2.2)$$

$$\hat{w}(a, \phi) = 1 \quad \phi > 0 \quad (2.3)$$

$$\frac{\partial \hat{w}}{\partial r}(0, \phi) = 0 \quad \phi \geq 0 \quad (2.4)$$

Wedemeyer derived a partial differential equation for $\hat{w}(r, \phi)$ which was numerically integrated by Sedney and Gerber.¹² The equation has the following form:

$$\frac{\partial \hat{w}}{\partial \phi} + \hat{V} \left[2 \hat{w} + r \frac{\partial \hat{w}}{\partial r} \right] = \frac{a^2}{\text{Re}} \left[\frac{\partial^2 \hat{w}}{\partial r^2} + (3/r) \left(\frac{\partial \hat{w}}{\partial r} \right) \right] \quad (2.5)$$

* The proper numerical way to treat these discontinuous conditions is given in Reference 17.

17. R. Sedney and N. Gerber, "Treatment of the Discontinuity in the Spin-Up Problem with Impulsive Start," Ballistic Research Laboratory, Aberdeen Proving Ground, Maryland, BRL Technical Report ARBRL-TR-02520, September 1983. (AD A133682)

where

$$\hat{V} = -k_{\ell} (1 - \hat{w}) \quad \text{laminar Ekman layers}$$

$$= -k_t (1 - \hat{w})^{8/5} (r/a)^{3/5} \quad \text{turbulent Ekman layers}$$

$$k_{\ell} = \kappa (a/c) (Re)^{-1/2}; \quad \kappa \text{ is usually } 0.5$$

$$k_t = .035 (a/c) Re^{-1/5}$$

$$Re = \frac{a^2 \dot{\phi}}{\nu}$$

Wedemeyer derived a very simple laminar Ekman layer solution which has a discontinuity in shear at an interior point.

$$\left. \begin{aligned} \hat{w} &= 0 & r &\leq r_f \\ & & r_f &\leq r \leq a \end{aligned} \right\} \quad (2.6)$$

$$= \frac{1 - (r_f/r)^2}{1 - (r_f/a)^2}$$

where

$$r_f = a e^{-k_{\ell} \phi}$$

According to this solution, the flow field is divided into two regions: an inner core flow which is stationary and an outer rotating flow. The boundary $r = r_f$ is an inward moving front where the velocity has discontinuous derivatives. A numerical solution to Eq. (2.5), of course, does not have this discontinuity. r_f , however, is a useful measure of the extent of the spin-up process. Laminar Ekman layer solutions of Eq. (2.5) have been computed for $Re = 40,000$, $c/a = 4.0$ and are compared for an early time, $\phi = 800$ rad ($r_f = .6$) in Figure 1 and for a late time, $\phi = 2600$ rad ($r_f = .2$) in Figure 2. The extent of spin-up can be described by the ratio of the liquid angular momentum to the fully spin-up liquid angular momentum:

$$I = \left(\frac{4}{a^4} \right) \int_0^a r^3 \hat{w} dr \quad (2.7)$$

In Figure 3, I is plotted versus ϕ/\sqrt{Re} for several conditions. Note that for larger Reynolds numbers, spin-up requires many more revolutions - i.e., much

more flight time. For $\dot{\phi} = 1000 \text{ s}^{-1}$, the liquid angular momentum is 95% of that of a rigid body in 1.6 seconds for laminar Ekman layers ($Re = 40,000$) and in 9 seconds for turbulent Ekman layers ($Re = 10^6$).

We now assume that velocity components and pressure can be expressed in a more general form than that used in Reference 3.

$$V_x = R \left\{ u_s e^{s\phi - im\theta} \right\} (a\dot{\phi}) \quad (2.8)$$

$$V_r = R \left\{ v_s e^{s\phi - im\theta} \right\} (a\dot{\phi}) \quad (2.9)$$

$$V_\theta = r\dot{\phi} \hat{w} + R \left\{ w_s e^{s\phi - im\theta} \right\} (a\dot{\phi}) \quad (2.10)$$

$$P = \rho_L a^2 \dot{\phi}^2 \hat{p} + R \left\{ p_s e^{s\phi - im\theta} \right\} (\rho_L a^2 \dot{\phi}^2) \quad (2.11)$$

where
$$\hat{p} = a^{-2} \int_0^r [\hat{w}(r_1)]^2 r_1 dr_1 \quad (2.12)$$

$$m = 0, \pm 1, \pm 2 \dots$$

The basic flow, $\hat{w}(r, \phi)$, is a function of time ($\phi = \dot{\phi}t$); but we will assume slow variation with time in comparison with the frequency of the coning motion.

For positive spin, the linearized Navier-Stokes equations become

$$(s - m \hat{w} i) v_s - 2\hat{w} w_s + a \frac{\partial p_s}{\partial r} = Re^{-1} \left[\nabla_\theta^2 v_s - (v_s - 2 m i w_s) a^2/r^2 \right] \quad (2.13)$$

$$(s - m \hat{w} i) w_s + \left(2\hat{w} + r \frac{\partial \hat{w}}{\partial r} \right) v_s - im a p_s/r$$

$$= Re^{-1} \left[\nabla_\theta^2 w_s - (w_s + 2 i m v_s) a^2/r^2 \right] \quad (2.14)$$

$$(s - m \hat{w} i) u_s + a \frac{\partial p_s}{\partial x} = Re^{-1} \nabla_{\theta}^2 u_s \quad (2.15)$$

$$\frac{\partial (r v_s)}{\partial r} - m w_s i + r \frac{\partial u_s}{\partial x} = 0 \quad (2.16)$$

where

$$\nabla_{\theta}^2 = a^2 \left[\frac{\partial^2}{\partial r^2} + \frac{\partial}{r \partial r} + \frac{\partial^2}{\partial x^2} - \frac{m^2}{r^2} \right] \quad (2.17)$$

Next we assume the perturbation variables, u_s , v_s , w_s , p_s are not affected by the Ekman layers and Stewartson layer and must satisfy the boundary conditions independently by means of their own boundary layers. This assumption is clearly somewhat arbitrary but allows us to get a first estimate of the effect of spin-up flow on the coning motion. This will be refined in the future as our understanding of the fluid mechanics improves.

The payload is assumed to be in coning motion described by:

$$\hat{\beta} + i \hat{\alpha} = \hat{K} e^{s\phi} \quad (2.18)$$

where $\hat{K} = K_{10} e^{i\phi_{10}}$; $s = (\epsilon + i) \tau$

Since (x, r, θ) are cylindrical coordinates in an inertia non-coning axis system, it is convenient to introduce cylindrical coordinates $(\hat{x}, \hat{r}, \hat{\theta})$ in an aeroballistic axis system that cones with the projectile. The linear relations between these coordinates are:

$$\hat{x} = x - R \left\{ r \hat{K} e^{s\phi} - i\theta \right\} \quad (2.19)$$

$$\hat{r} = r + R \left\{ x \hat{K} e^{s\phi} - i\theta \right\} \quad (2.20)$$

$$\hat{\theta} = \theta - R \left\{ i (x/r) \hat{K} e^{s\phi} - i\theta \right\} \quad (2.21)$$

In the aeroballistic coordinates the walls of a cylindrical container whose center is at the projectile's center of mass have the simple coordinates $\hat{r} = a$ and $\hat{x} = \pm c$. At these surfaces the liquid velocity components must equal the wall velocity components:

$$\left. \begin{aligned} u_s &= (s - i) (r/a) \hat{K} \\ v_s &= -(s - i) (x/a) \hat{K} \end{aligned} \right\} (m = 1) \quad (2.22)$$

$$w_s = \left[1 + is + \hat{r} \frac{\partial \hat{w}(\hat{r})}{\partial \hat{r}} \right] (x/a) \hat{K}$$

$$u_s = v_s = w_s = 0 \quad (m \neq 1) \quad (2.23)$$

The perturbation variables are separated into inviscid and viscous components where the viscous components are solved by boundary layer approximations:

$$u_s = u_{si} + u_{sv} \quad (2.24)$$

$$v_s = v_{si} + v_{sv} \quad (2.25)$$

$$w_s = w_{si} + w_{sv} \quad (2.26)$$

$$p_s = p_{si} + p_{sv} \quad (2.27)$$

For the fully spun-up liquid, the boundary layer analysis leads to the following boundary condition for the inviscid flow.

$$\left. \begin{aligned} \left[v_{si} - a \delta_a \frac{\partial v_{si}}{\partial r} \right]_{r=a} &= (i-s) (x/a) \hat{K} & (m = 1) \\ &= 0 & (m \neq 1) \end{aligned} \right\} \quad (2.28)$$

$$\left. \begin{aligned} \left[u_{si} \mp c \delta_c \frac{\partial u_{si}}{\partial x} \right]_{x=\pm c} &= (s - i) (r/a) \hat{K} & (m = 1) \\ &= 0 & (m \neq 1) \end{aligned} \right\} \quad (2.29)$$

where

$$\delta_a = \frac{1+i}{\sqrt{2(m+is)}} \operatorname{Re}^{-1/2} \quad (2.30)$$

$$\delta_c = -[2(m+is)]^{-1} [(2-m-is) \alpha^{-1} - (2+m+is) \beta^{-1}] \quad (2.31)$$

$$\alpha = (c/a) [s - (2+m)i]^{1/2} \operatorname{Re}^{1/2} \quad (2.32)$$

$$\beta = (c/a) [s + (2-m)i]^{1/2} \operatorname{Re}^{1/2} \quad (2.33)$$

and the complex roots are selected to have positive real parts. δ_a and δ_c are complex parameters whose real parts act like displacement thicknesses, as can be seen from Eqs. (2.28 - 2.29). Their imaginary parts indicate time lags in the fluid response to the periodic wall motion.

During spin-up, the lateral wall boundary layer has the same Reynolds number and is essentially unaffected, but the end wall boundary layer has an exterior flow of $r\hat{w}\hat{\phi}$ rather than $r\hat{\phi}$. As a crude approximation, we will assume Eq. (2.28) still applies during spin-up and the Reynolds number in Eq. (2.29) should be modified by an average \hat{w} .

$$\left[u_{si} \mp (\hat{w}_a)^{-1/2} c \delta_c \frac{\partial u_{si}}{\partial x} \right]_{x=\pm c} = \begin{cases} (s-i)(r/a) \hat{K} & m=1 \\ 0 & m \neq 1 \end{cases} \quad (2.34)$$

where

$$\hat{w}_a = \frac{2}{a^2} \int_0^a \hat{w} r dr \quad (2.35)$$

The inviscid velocity components satisfy Eqs. (2.13 - 2.15) for infinite Reynolds number.

$$u_{si} = -a (s - m \hat{w} i)^{-1} \frac{\partial p_{si}}{\partial x} \quad (2.36)$$

$$v_{si} = \left[2 i (a/r) m \hat{w} p_{si} - (s - m \hat{w} i) a \frac{\partial p_{si}}{\partial r} \right] D^{-1} \quad (2.37)$$

$$w_{si} = \left[i (a/r) m (s - m \hat{w} i) p_{si} + \left(2 \hat{w} + r \frac{\partial \hat{w}}{\partial r} \right) a \frac{\partial p_{si}}{\partial r} \right] D^{-1} \quad (2.38)$$

where

$$D = s^2 - 2 m \hat{w} s i + (4 - m^2) \hat{w}^2 + r \frac{\partial (\hat{w}^2)}{\partial r} \quad (2.39)$$

Eqs. (2.36 - 2.38) can now be substituted in Eq. (2.16) to yield a differential equation for p_{si} .

$$\begin{aligned} \frac{\partial^2 p_{si}}{\partial r^2} + r^{-1} \left[1 - r \frac{\partial D}{\partial r} D^{-1} \right] \frac{\partial p_{si}}{\partial r} \\ - r^{-2} \left[m^2 + 2 m r i (s - m \hat{w} i)^{-1} D \frac{\partial (\hat{w}/D)}{\partial r} \right] p_{si} \\ = - (s - m \hat{w} i)^{-2} D \frac{\partial^2 p_{si}}{\partial x^2} \end{aligned} \quad (2.40)$$

Next we make the usual assumption that p_{si} is a sum of products of functions of r and functions of x :

$$p_{si} = \sum R_k (r) X_k (x) \quad (2.41)$$

$$X_k'' + c^{-2} \lambda_k^2 X_k = 0 \quad (2.42)$$

$$R_k'' + r^{-1} \left[1 - r \frac{\partial D}{\partial r} D^{-1} \right] R_k' \quad (2.43)$$

$$- r^{-2} \left[m^2 - r^2 c^{-2} \lambda_k^2 + 2 m r i (s - m \hat{w} i)^{-1} D \frac{\partial (\hat{w}/D)}{\partial r} \right] R_k = 0$$

$$\text{where } \hat{\lambda}_k^2 = - (s - m \hat{w} i)^{-2} D \lambda_k^2 \quad (2.44)$$

and λ_k is a constant. If the constant is zero, k will be assigned the value of zero, i.e., $\lambda_0 = 0$. The solutions to Eq. (2.42) are

$$X_0 = A_0 + B_0 (x/c) \quad (2.45)$$

$$X_k = A_k \cos (\lambda_k x/c) + B_k \sin (\lambda_k x/c) \quad k \neq 0, \quad (2.46)$$

For constant \hat{w} and $k \neq 0$, Eq. (2.43) becomes Bessel's equation. For a fully-filled container, p_{sj} must be bounded for $r = 0$ and so only Bessel functions of the first kind need be considered.

$$R_k = C J_m (\hat{\lambda}_k r/c) \quad k \neq 0 \quad (2.47)$$

where J_m is the Bessel function of the first kind of order m and C is an arbitrary constant. (A convenient choice for C is 1.) For varying \hat{w} , the numerical solution of Eq. (2.43) for $k \neq 0$ is R_k where

$$R_k (r) \rightarrow \begin{cases} f (r) \\ (-1)^m f (r) \end{cases} \text{ as } r \rightarrow 0 \quad \begin{array}{l} m \geq 0 \\ m \leq 0 \end{array} \quad (2.48)$$

where

$$f (r) = C \left[(r/c) \hat{\lambda}_{k0} \right]^{\hat{m}} / (2^{\hat{m}} \hat{m}!)$$

$$\hat{m} = |m|$$

$$\hat{\lambda}_{k0} = \left[\hat{\lambda}_k \right]_{r=0}$$

These conditions on R_k are selected so that it reduces to Eq. (2.47) for constant \hat{w} .

III. EIGENVALUES

The solution for the perturbation functions can be written as the sum of a steady-state response to the coning motion and a transient solution for which $\hat{K} = 0$ in the boundary conditions (Eqs.(2.28, 2.34)). The steady-state solution only involves perturbation functions for $m = 1$ while the transient solutions can have any integer value of m in the homogeneous boundary conditions. The homogeneous version of Eq. (2.34) yields a very simple condition for λ_k when $\lambda_k \delta_c$ is small. (See page 97 of Reference 3 for exact relations.)

$$\lambda_k = k (\pi/2) [1 + (w_a)^{-1/2} \delta_c] \quad (3.1)$$

The homogeneous Eq. (2.28), however, with Eq. (2.37) imposes a more complicated requirement on $R_k(r)$:

$$R_{kv}(a,s) - a \delta_a \frac{\partial R_{kv}}{\partial r}(a,s) = 0 \quad (3.2)$$

where*

$$R_{kv}(r,s) = [(s - m \hat{w} i) a R_k'(r) - 2 m (a/r) \hat{w} i R_k(r)] D^{-1}(r,s) \quad (3.3)$$

Values of s that satisfy Eq. (3.2) are the eigenvalues, s_{kn} , and the corresponding $\lambda_k R_k$ products are the eigenvectors. For a stable steady-state solution, these functions should decay to zero, which requires $\text{Re } s_{kn} < 0$.

A fairly straight-forward iteration can be used to find the s_{kn} except near singularities of Eq. (2.43), i.e., when

$$s = m \hat{w} i \quad (3.4)$$

Since s_{kn} is primarily imaginary, $i \tau_{kn}$, this condition for the critical radius, $r = r_c$, is approximately

$$\tau_{kn} = m \hat{w} (r_c, \phi) \quad (3.5)$$

*The subscript "v" identifies the function of R_k that is used in computing v_{si} .

According to Eq. (3.5), the critical layer is located where the liquid angular velocity is τ/m and an internal resonance occurs. For an inviscid calculation, very large perturbation functions result; and the much more complete linearized Navier-Stokes method is necessary. For any fixed time, the minimum value of \hat{w} is its value at $r = 0$, i.e., $\hat{w}_0 = \hat{w}(0, \phi)$. For a large portion of the spin-up period, \hat{w}_0 is zero and then it grows to unity, which indicates a fully spun-up condition. In Figure 4, spin angles for which \hat{w}_0 is 0.11 are plotted versus Reynolds number. Since projectile coning frequencies are usually less than 0.10, this figure allows us to make estimates for the region of validity of the theory of this paper. At a Reynolds number of 40,000, for example, critical layers should not exist at projectile coning frequencies for spin angles greater than 1200 rad. For a spin rate of 1000 rad/s, this means that the theory of this report should apply after 1.2 seconds of flight.

IV. STEADY-STATE SOLUTION

Since the boundary conditions (Eq. (2.22)) imposed by the forcing function are specified for $m = 1$, the steady-state solution will also have $m = 1$. In order to satisfy these inhomogeneous boundary conditions, we will express p_{si} by a $\lambda_k = 0$ term plus two series of products of functions of x and of r .

$$p_{si} = p_0 + p_\ell + p_e \quad (4.1)$$

$$= -(c/a) \left[R_{e0} X_0 + \sum_{k=1}^{N_\ell} d_{\ell k} R_{\ell k}(r) X_{\ell k}(x) + \sum_{n=1}^{N_e} d_{en} R_{en}(r) X_{en}(x) \right] \hat{K}$$

where $X_0 = A_0 + B_0 (x/c)$

R_{e0} is the solution of Eq. (2.43) for $\lambda_k = 0$,

$$R_{e0}(0) = 0; R_{e0}(a) = 1,$$

$$X_{\ell k} = A_{\ell k} \cos(\lambda_{\ell k} x/c) + B_{\ell k} \sin(\lambda_{\ell k} x/c),$$

$$X_{en} = A_{en} \cos(\lambda_{en} x/c) + B_{en} \sin(\lambda_{en} x/c),$$

$R_{\ell k}, R_{en}$ are solutions of Eq. (2.43) for $m = 1$, $\lambda_k = \lambda_{\ell k}$ or λ_{en} , respectively, and $R_k(0) = 0$, a $R_k'(0) = 1/a$.

The velocity components u_{sj} , v_{sj} , and w_{sj} can be computed from Eq. (4.1) by use of Eqs. (2.36 - 2.38).

$$u_{sj} = (s - \hat{w} i)^{-1} \left[B_0 R_{eo} + c \sum_{k=1}^{N_\ell} d_{\ell k} R_{\ell k} X'_{\ell k} + c \sum_{n=1}^{N_e} d_{en} R_{en} X'_{en} \right] \hat{K} \quad (4.2)$$

$$v_{sj} = (c/a) \left[R_{eov} X_0 + \sum d_{\ell k} R_{\ell kv} X_{\ell k} + \sum d_{en} R_{env} X_{en} \right] \hat{K} \quad (4.3)$$

$$w_{sj} = (c/a) \left[R_{eow} X_0 + \sum d_{\ell k} R_{\ell kw} X_{\ell k} + \sum d_{en} R_{enw} X_{en} \right] \hat{K} \quad (4.4)$$

where, if $G(r)$ denotes $R_{eo}(r)$, $R_{\ell k}(r)$ or $R_{en}(r)$, we have

$$G_v(r) = \left\{ [s - i \hat{w}(r)] a G'(r) - 2 i (a/r) \hat{w}(r) G(r) \right\} D^{-1}(r) ;$$

$$G_w(r) = - \left[\left(2\hat{w} + r \frac{\partial \hat{w}}{\partial r} \right) a G'(r) + i (a/r) (s - i\hat{w}) G(r) \right] D^{-1}(r) .$$

The first series will be constructed to satisfy the inhomogeneous boundary condition on the lateral wall (Eq. (2.28)) and the second series, the inhomogeneous boundary conditions (Eq. (2.34)) on the end walls. Each series will also be constrained to have no effect on the boundary conditions on the other walls. This means the first series must satisfy the homogeneous conditions at the end walls and the second series the homogeneous conditions at the lateral wall.

$$\therefore X'_{\ell k}(\pm c) \mp c (\hat{w}_a)^{-1/2} \delta_c X''_{\ell k}(\pm c) = 0 \quad (4.5)$$

$$R_{env}(a,s) - a \delta_a \frac{\partial R_{env}(a,s)}{\partial r} = 0 \quad (4.6)$$

Eq. (4.5) imposes simple conditions on $\lambda_{\ell k}$ and the $A_{\ell k}$'s.

$$\left. \begin{aligned} \lambda_{\ell k} &= (\pi k/2) [1 + (\hat{w}_a)^{-1/2} \delta_c] \\ A_{\ell k} &= 0 && k \text{ odd} \\ B_{\ell k} &= 0. && k \text{ even} \end{aligned} \right\} \quad (4.7)$$

Next, we expand (x/c) in a finite series in $\sin(\lambda_{\ell k} x/c)$:

$$x/c = \sum_{k=1}^{N_\ell} a_{\ell k} \sin(\lambda_{\ell k} x/c) \quad k \text{ odd} \quad (4.8)$$

The coefficients can be determined by a least squares fit.³

$$\sum_{k=1}^{N_\ell} b_{jk} a_{\ell k} = b_j \quad k, j \text{ odd} \quad (4.9)$$

where

$$b_j = c^{-2} \int_{-c}^c x \sin(\bar{\lambda}_{\ell j} x/c) dx \quad (4.10)$$

$$b_{jk} = c^{-1} \int_{-c}^c \sin(\bar{\lambda}_{\ell j} x/c) \sin(\lambda_{\ell k} x/c) dx \quad (4.11)$$

X_0 can now be expressed in terms of $\sin(\lambda_k x/c)$.

$$X_0(x) = A_0 + B_0 \sum_{k=1}^{N_\ell} a_{\ell k} \sin(\lambda_k x/c) \quad (4.12)$$

Equations (4.1, 4.12) can be used in conjunction with Eq. (2.37) to compute v_{sj} and $\frac{\partial v_{sj}}{\partial r}$ at $r = a$ as a sum of terms involving 1, $\sin(\lambda_{\ell k} x/c)$, $\cos(\lambda_{\ell k} x/c)$ and X_{en} , all of whose coefficients are functions of r . These expressions can be combined with Eq. (4.8) in the lateral wall boundary condition (Eq. (2.28)). Terms in X_{en} drop out due to Eq. (4.6), and the conditions on A_0 , $A_{\ell k}$ and $B_{\ell k}$ can be obtained.

$$A_0 = 0 \quad (4.13)$$

$$d_{\ell k} \left[R_{\ell k v} - a \delta_a \frac{\partial R_{\ell k v}}{\partial r} \right]_{r=a} = a_{\ell k} F; \quad B_{\ell k} = 1, \quad k \text{ odd} \quad (4.14)$$

$$A_{\ell k} = 0 \quad k \text{ even} \quad (4.15)$$

where

$$F = i - s - B_0 \left[R_{eov} - a \delta_a \frac{\partial R_{eov}}{\partial r} \right]_{r=a}$$

The expressions for p_0 and p_ℓ are now considerably simpler.

$$p_0 = -B_0 (x/a) R_{e0}(r) \quad (4.16)$$

$$p_\ell = -(c/a) \sum_{k=1}^{N_\ell} d_{\ell k} R_{\ell k}(r) \sin(\lambda_{\ell k} x/c) \quad k = 1, 3, 5 \dots \quad (4.17)$$

The construction of the p_e series and the determination of B_0 is somewhat more complicated. The primary difficulty is the determination of the λ_{en} 's. These are the eigenvalues that satisfy Eq. (4.3). The subscript n identifies

the eigenvalues in order of increasing size. These eigenvalues can be found by an iterative process. The first guess for these can be obtained from a table of inviscid eigenfrequencies such as Table 3 of Reference 3. In this table, the eigenfrequencies τ_{nk} are tabulated as functions of a reduced fineness ratio, f^* .

$$\tau_{nk} = F_n (f^*) \quad (4.18)$$

$$\text{where } f^* = c/ka = \pi c/2\lambda_k a \quad (4.19)$$

These tables are constructed by finding pairs of τ_{nk} 's and λ_k 's that satisfy Eq. (4.3) for $\delta_a = 0$. Thus, for a specific frequency $\tau = \tau_{nk}$, each of the F_n functions can specify a wave number $\lambda_{en} = \lambda_k$ that satisfies Eq. (2.43). For example, for $\tau = .04$, and $c/a = 3$, $\lambda_{e1} = 4.524$, $\lambda_{e2} = 9.364$, $\lambda_{e3} = 14.405$.

Equation (4.2) can now be used in boundary conditions (2.34) to yield

$$A_{en} = 0 \quad B_{en} = 1 \quad n \neq 0 \quad (4.20)$$

$$B_0 R_{e0} + c \sum_{n=1}^{N_e} d_{en} \lambda_{en} [\cos \lambda_{en} + (w_a)^{-1/2} \delta_a \lambda_{en} \sin \lambda_{en}] R_{en} = (s - i)^2 g(r) \quad (4.21)$$

$$\text{where } g(r) = \left[\frac{s - i \hat{w}(r)}{s - i} \right] (r/a)$$

Next we fit $g(r)$ to a series in the R_{en} 's by use of least squares.

$$g(r) = \sum_{n=0}^{N_e} a_{en} R_{en} \quad (4.22)$$

$$\text{where } \sum_{n=0}^{N_e} c_{jn} a_{en} = c_j \quad j = 0, 1, \dots, N_e \quad (4.23)$$

$$c_j = a^{-1} \int_0^a g(r) \bar{R}_{ej} dr \quad (4.24)$$

$$c_{jn} = a^{-1} \int_0^a \bar{R}_{ej} R_{en} dr \quad (4.25)$$

Eqs. (4.21-4.22) can now be combined to give conditions on B_0 and d_{en} .

$$B_0 = (s - i)^2 a_{e0} \quad (4.26)$$

$$d_{en} \lambda_{en} [\cos \lambda_{en} + (w_a)^{-1/2} \delta_c \lambda_{en} \sin \lambda_{en}] = (s - i)^2 a_{en} \quad n \neq 0 \quad (4.27)$$

For a fully spun-up liquid, R_{e0} is r/a , $a_{e0} = 1$, $a_{en} = 0$ ($n \neq 0$), $p_e = 0$, and the solution reduces to that of Reference 3. When the liquid is not fully spun-up, the a_{en} 's are not zero but are moderately small. Only when the expression in brackets is small does d_{en} become large. This is the case when λ_{en} is near a λ_{ek} .

V. LIQUID MOMENT

The linear liquid moment in response to the coning motion described by Eq. (2.13) can be expressed in the following form in terms of the non-spinning aeroballistic axis system, $\tilde{X}, \tilde{Y}, \tilde{Z}$ which pitches and yaws with the missile.

$$M_{LY} + i M_{LZ} = m_L a^2 \dot{\phi}^2 \tau (C_{LSM} + i C_{LIM}) \hat{K} e^{S\phi} \quad (5.1)$$

The imaginary part of the dimensionless moment coefficient, C_{LIM} , causes a rotation in the plane of the coning moment and is called the liquid in-plane moment coefficient while the real part, C_{LSM} , causes a rotation out of this plane and is called the liquid side moment coefficient. Since C_{LSM} affects the damping of the coning motion, and C_{LIM} only affects the frequency, prediction of C_{LSM} is the primary objective of any theory.

The major components of the liquid moment are due to the pressure on the lateral and end walls of the container. Lesser components are due to the viscous wall shear on the lateral and end walls; thus, the liquid moment coefficient can be given as the sum of four terms:

$$\tau (C_{LSM} + i C_{LIM}) = m_{p\ell} + m_{pe} + m_{v\ell} + m_{ve} \quad (5.2)$$

The pressure as given by Eq. (2.11) is specified as a function of r and x . Eqs. (2.19 - 2.20) can be used to yield a linear approximation for pressure as a function of \tilde{r} and \tilde{x} .

$$\begin{aligned}
p (p_L \dot{\phi} a^2)^{-1} &= \hat{p}(\hat{r}) + \frac{d\hat{p}}{d\hat{r}} (r - \hat{r}) + R \left\{ p_s e^{s\phi - i\theta} \right\} \\
&= \hat{p}(\hat{r}) + R \left\{ \left[p_s - \frac{\hat{x} \hat{r} \hat{\omega}^2 \hat{K}}{a^2} \right] e^{s\phi - i\theta} \right\}
\end{aligned} \tag{5.3}$$

The pressure moments relative to the center of the cylinder are:

$$\begin{aligned}
\therefore m_{p\ell} &= i(2\pi a c \hat{K})^{-1} e^{-s\phi} \int_{-c}^c \int_0^{2\pi} \hat{x} e^{i\hat{\theta}} R \left\{ \left[p_s - (\hat{x}/a) \hat{K} \right] e^{s\phi - i\theta} \right\} d\hat{x} d\hat{\theta} \\
&= i(2ac)^{-1} \int_{-c}^c \hat{x} \left[p_s(a, \hat{x}) \hat{K}^{-1} - (\hat{x}/a) \right] d\hat{x}
\end{aligned} \tag{5.4}$$

and

$$m_{pe} = -i(a^2 c)^{-1} \int_0^a \left[p_s(\hat{r}, c) \hat{K}^{-1} - \hat{r} \hat{\omega}^2 (c/a^2) \right] \hat{r}^2 d\hat{r} \tag{5.5}$$

The viscous components of the liquid moment are computed by the formula (7.2, 7.3) of Reference 3 and are given in Appendix A.

VI. NUMERICAL CALCULATIONS

In Reference 16, Navier-Stokes calculations of eigenfrequencies are given for $m = 0$, $Re = 43,000$ and for $m = 1$, $Re = 5000, 30,000, 40,000, 50,000, 2 \times 10^6$. δ_c was taken to be zero, and laminar Ekman layers were assumed for all cases except for Re of 2×10^6 which involved turbulent Ekman layers. The rotational symmetric case with $m = 0$ is given in Table 1. The degree of spin-up is indicated by r_f/a as defined in Eq. (2.6). This parameter varies from 1 to 0 as time varies from 0 to ∞ (fully spun-up). For this case, there is no critical layer; and the simple Linear-Boundary-Layer theory (LBL) gives the same frequencies as the numerically more difficult Navier-Stokes theory (NS). The damping rates do differ by .0005. Since the damping rates are determined by the viscosity on the cylindrical wall, this indicates the inaccuracy of the boundary layer approximation at this relatively low Reynolds number.

Table 2 gives results for the rotationally asymmetric case of $m = 1$. In the first part of this table, the eigenfrequencies for $n = 1$ are negative and, hence, no critical layer exists. Once again, the frequencies agree well although the comparison of the damping rates is much poorer. In the second part of the table, for $n = 2$, a critical layer does exist for $r_f/a = .27$ ($\hat{\omega}_0 = .02$)

Table 1. Comparison of Navier-Stokes and Linear-Boundary-Layer Eigenvalues for $m = 0$, $k = 2$, $c/a = .995$, $\kappa = .500$

Re = 43,000

n = 1

r_f/a	τ		ϵ	
	NS	LBL	NS	LBL
.221	1.202	1.201	-.0028	-.0023
.186	1.219	1.220	-.0027	-.0022
.133	1.242	1.243	-.0025	-.0020
.048	1.265	1.266	-.0023	-.0018
.009	1.268	1.269	-.0023	-.0018

Table 2. Comparison of Navier-Stokes and Linear-Boundary-Layer Eigenvalues for $m = 1$, $k = 1$, $c/a = .600$, $\kappa = .443$

r_f/a	τ		ϵ	
	NS	LBL	NS	LBL
(a) Re = 30,000, n = 1				
.300	-.3359	-.3355	.012	.010
.235	-.3707	-.3681	.010	.008
.026	-.4278	-.4282	.007	.006
(b) Re = 50,000, n = 2				
.271	.1526	.1540	-.021	-.00005
.202	.1648	.1642	-.018	-.012
.013	.1745	.1745	-.019	-.014

but the nonzero value of ϵ seems to be sufficient to allow a good evaluation of τ . The very small value of ϵ does indicate the nearness of an instability. The NS value of damping in the presence of a critical layer is a healthy value and shows the power of this method in the presence of a critical layer.

In Figure 5, the eigenfrequencies are compared for both laminar and turbulent Ekman layers and agreement is good for later spin-up. The Navier-Stokes values are, of course, the only ones appropriate for early spin-up. Finally, Figure 6 shows another comparison of eigenfrequencies for the very low Reynolds number of 4974 and the later spin-up values are in good agreement.

The LBL theory is the first to compute moment coefficients during spin-up. This is not an intrinsic limitation of the NS theory and approximate numerical codes are presently being developed for the Navier-Stokes theory. An example of the variation of the side moment coefficient with time is shown in Figure 7 for the conditions of the laminar Ekman layers curve of Figure 5. For the fixed coning frequency of .08, the side moment coefficient is computed for ϕ ranging from 1000 to 2000 rad. This covers the region between the disappearance of the critical layer and the establishment of a steady-state spin profile. As could have been predicted from Figure 5, the peak occurs at $\phi = 1400$ rad. This however, is the first calculation of the value of this peak side moment coefficient.

For the condition of Figure 7, the fully spun-up values of τ_{31} and its associated maximum C_{LSM} are .040 and .312. According to Figures 5 and 7, at $\phi = 1400$, these quantities are approximately .08 and .36. Thus, the peak side moment coefficient at this point of spin-up is 16% greater than its fully spun-up value.

In Figure 8, we plot the ratio of this maximum side moment coefficient to its value for $\phi = \infty$ versus ϕ . For the smallest value of ϕ for which the critical layer is not present, i.e., 1,000, the maximum side moment coefficient is 40% larger than its fully spun-up value. In this figure, the corresponding plot for $Re = 2 \times 10^6$ is also given. For the higher Reynolds number, the spin-up time is much larger and is in excess of 40,000. At the disappearance of the critical layer for ϕ of 7,000, the peak side moment coefficient is 30% less than its fully spun-up value. Finally in Figure 9, similar plots of the maximum side moment coefficient ratios are given for the conditions of Figure 6.

VII. SUMMARY

1. During the later portion of the spin-up process, the period of the circumferential flow is a function of radial distance from the spin axis but is never near the period of the coning motion, i.e., no critical layer exists.
2. For this time period, the simple linear boundary layer theory can be extended to compute eigenfrequencies and side moment coefficients.

3. The eigenfrequencies have been compared with those computed by the much more complicated Navier-Stokes perturbation method and excellent agreement has been obtained.

4. Side moment coefficients have been computed for critical layer free portion of the spin-up process and the maximum values corresponding to a particular eigenfrequency determined.

ACKNOWLEDGMENT

The theory of this report was programmed for the LFD VAX computer by James Bradley. Mr. Bradley's gifted work thereby transformed this theory from an academic exercise to a useful design tool. The author is particularly indebted to Mr. Bradley's patience as he adjusted his program to the many changes of the theory brought on by the author's increased understanding of the problem.

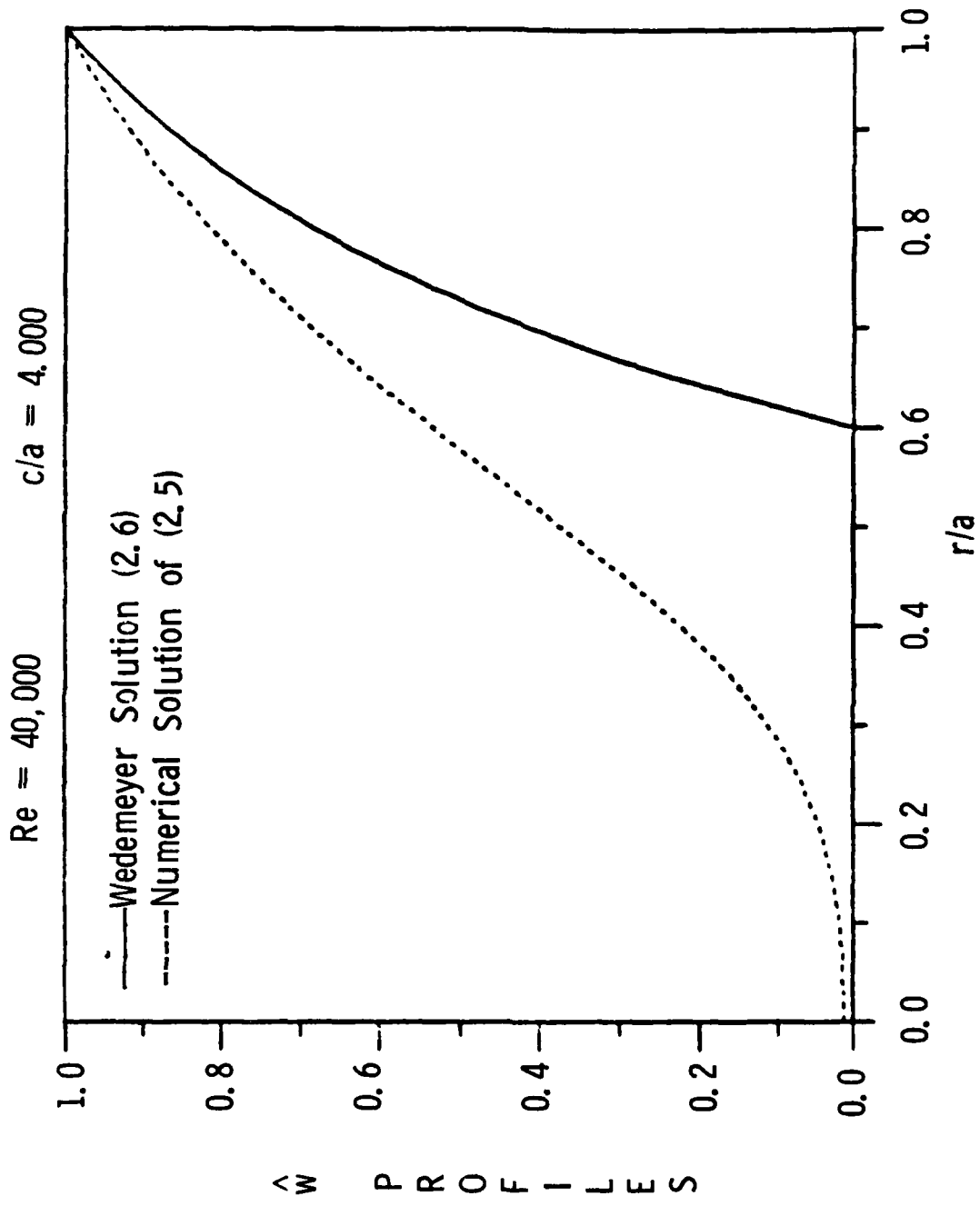


Figure 1. Laminar Flow Solutions of Eq. (2.5) for Re = 40,000, c/a = 4, $\phi = 800$ rad.

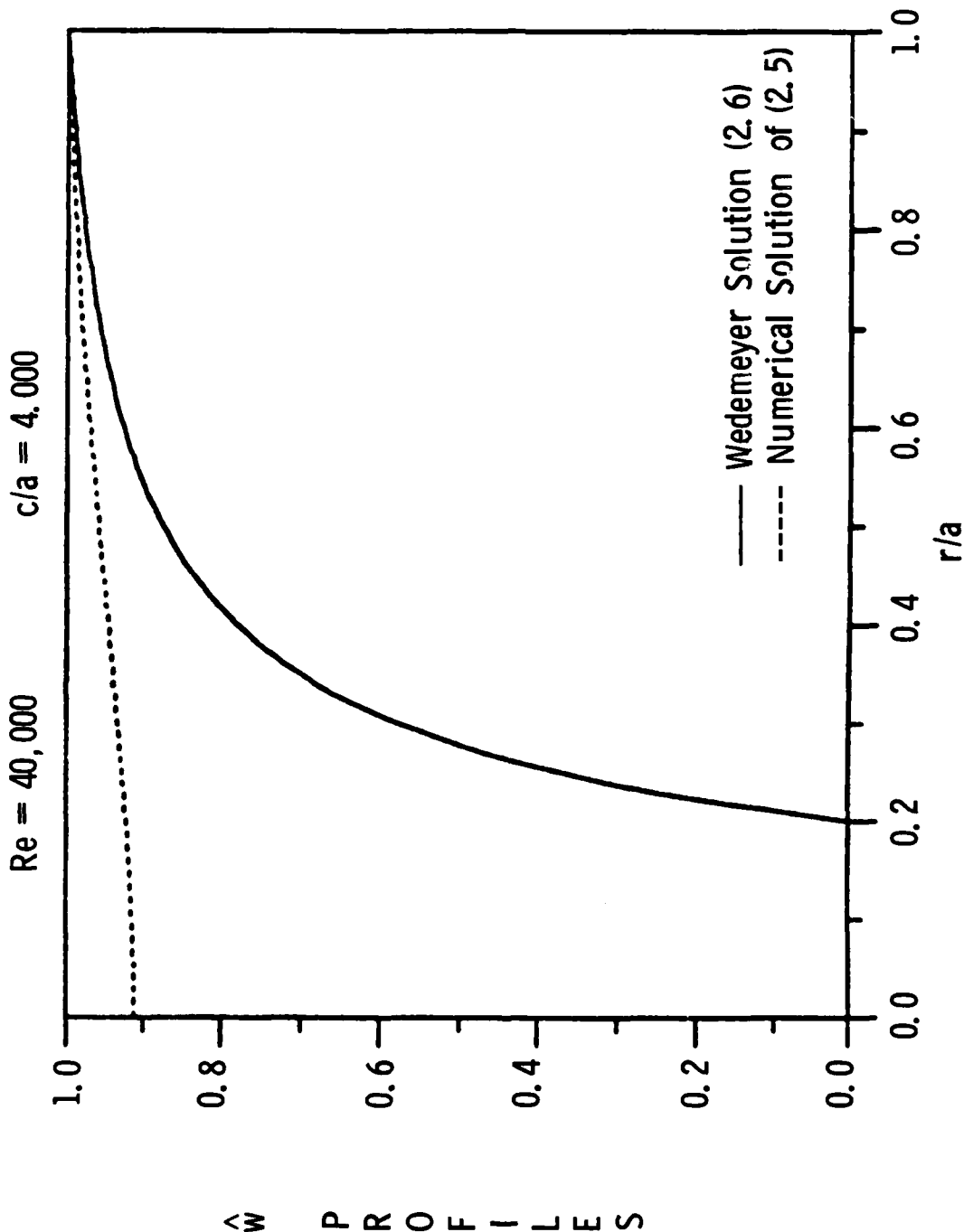


Figure 2. Laminar Flow Solutions of Eq. (2.5) for $Re = 40,000$, $c/a = 4$, $\phi = 2600$ rad.

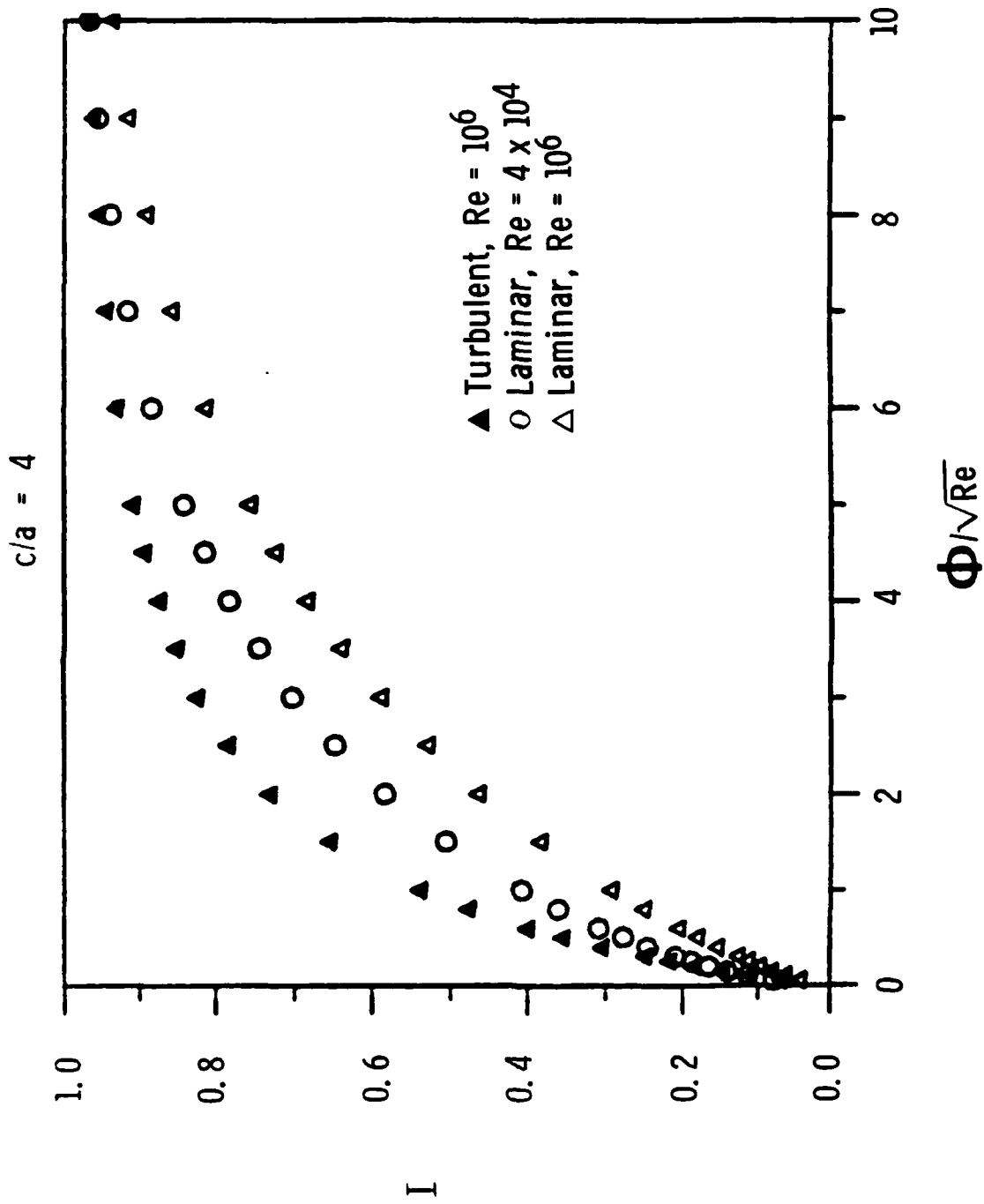


Figure 3. Liquid Angular Momentum Ratio vs Φ/\sqrt{Re} for $c/a = 4$.

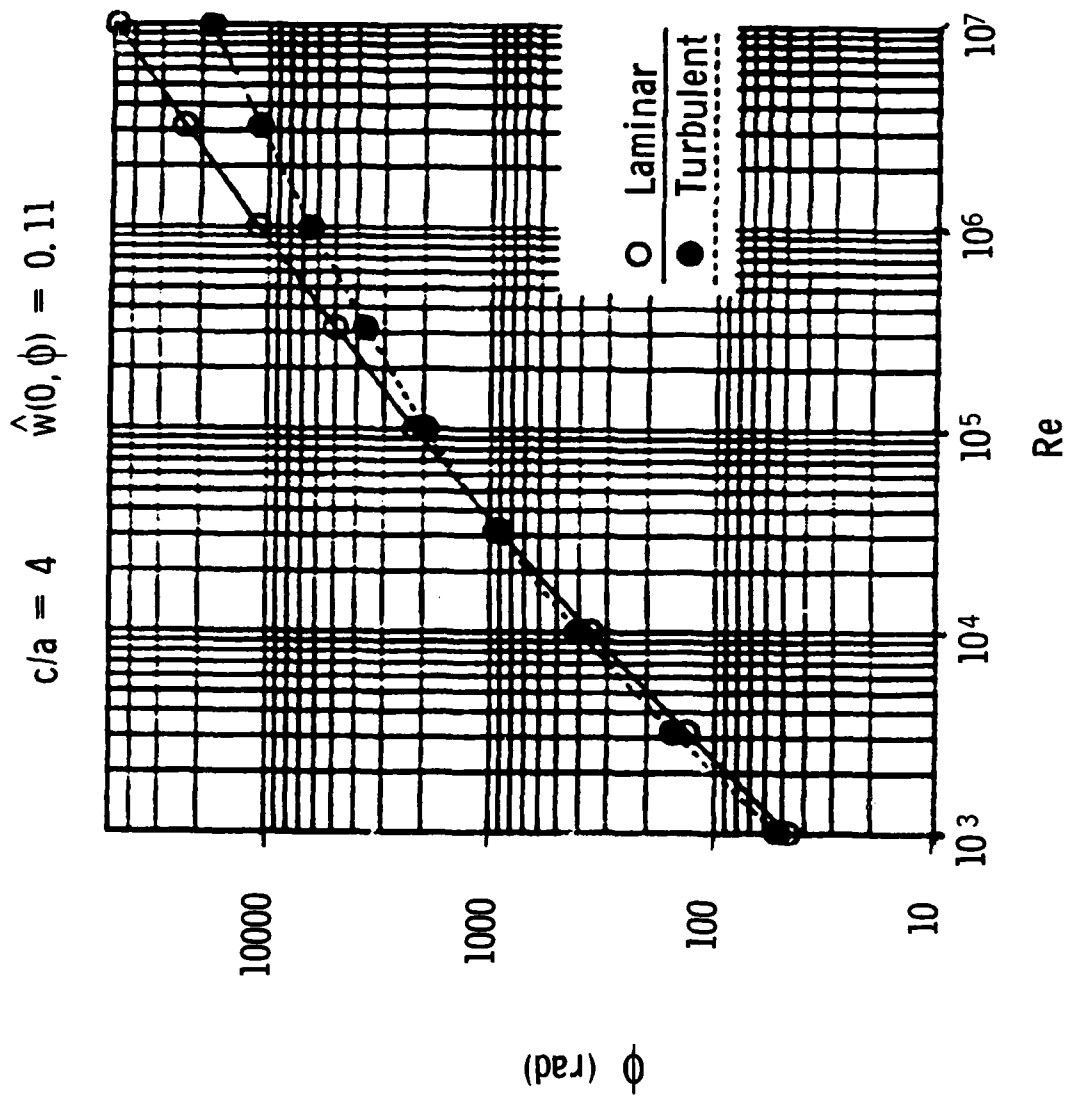


Figure 4. Spin Angles for which $\hat{w}_0 = 0.11$ vs Reynolds Number, $c/a = 4$.

$c/a = 3.120$

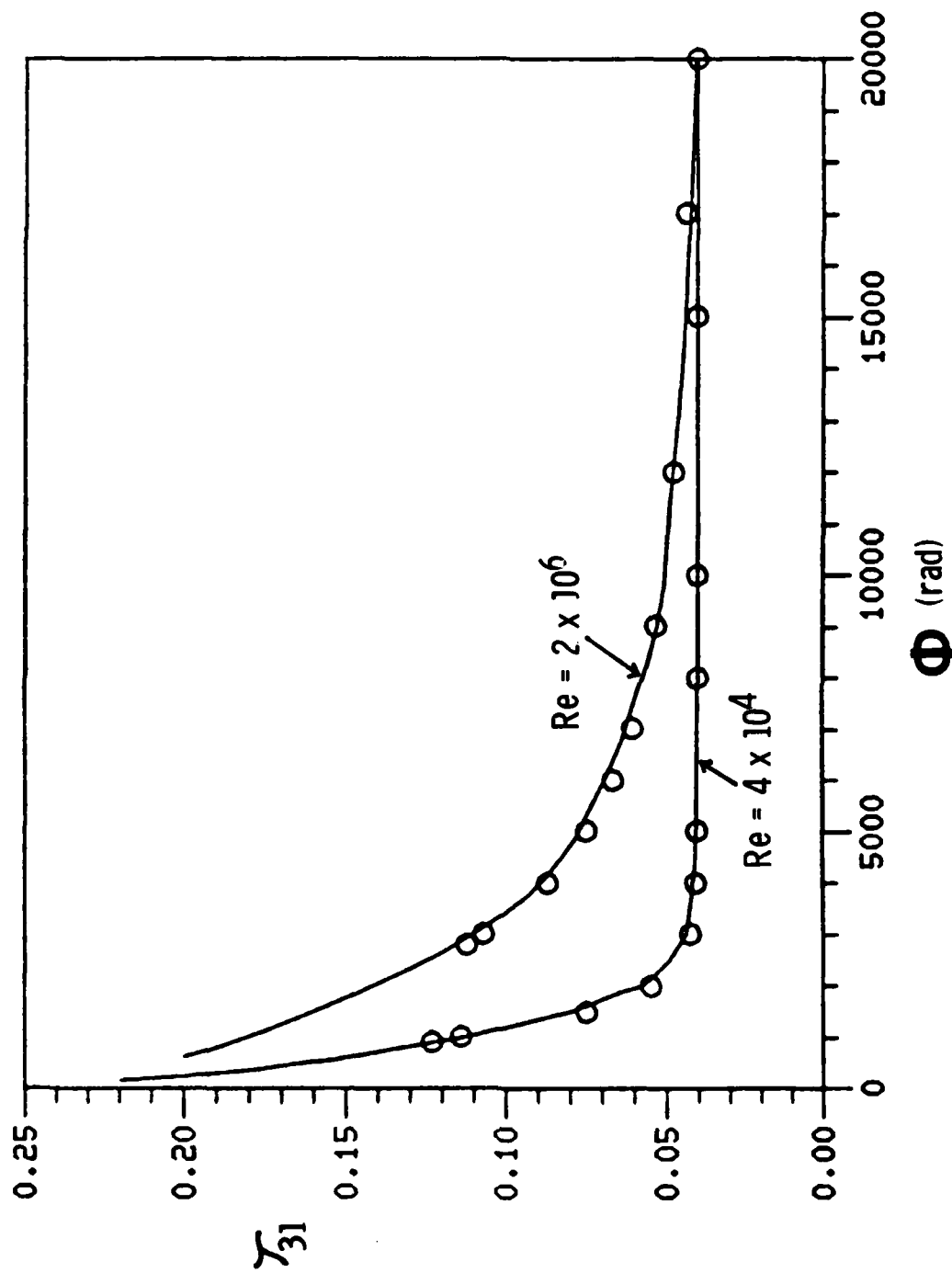


Figure 5. Eigenfrequency τ_{31} vs Spin Angle ϕ for $Re = 40,000$, $c/a = 3.12$, $k = 3$, $n = 1$, $\kappa = 0.443$. The Curves are from Sedney-Gerber NS Theory (Fig. 5, Ref. 16), the Circles are from Linear-Boundary-Layer Theory.

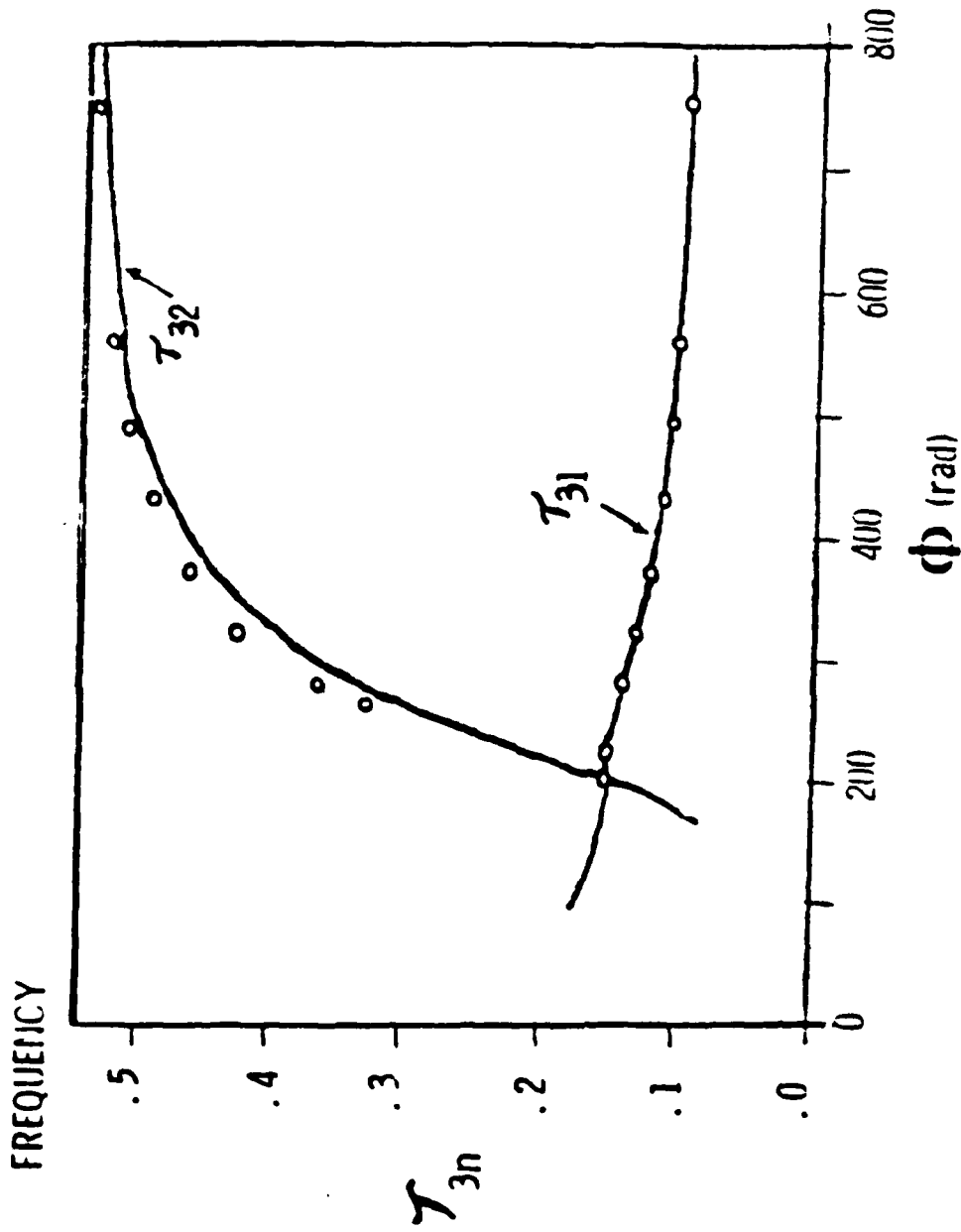


Figure 6. Eigenfrequency τ_{3n} vs Spin Angle ϕ for $Re = 5000$, $c/a = 3.297$, $k = 3$, $\kappa = 0.443$. The Curves are from Sedney-Gerber NS Theory (Fig. 6, Ref. 16), the Circles are from Linear-Boundary-layer Theory.

$Re = 40000, c/a = 3.12, \tau = .08, \kappa = .443$

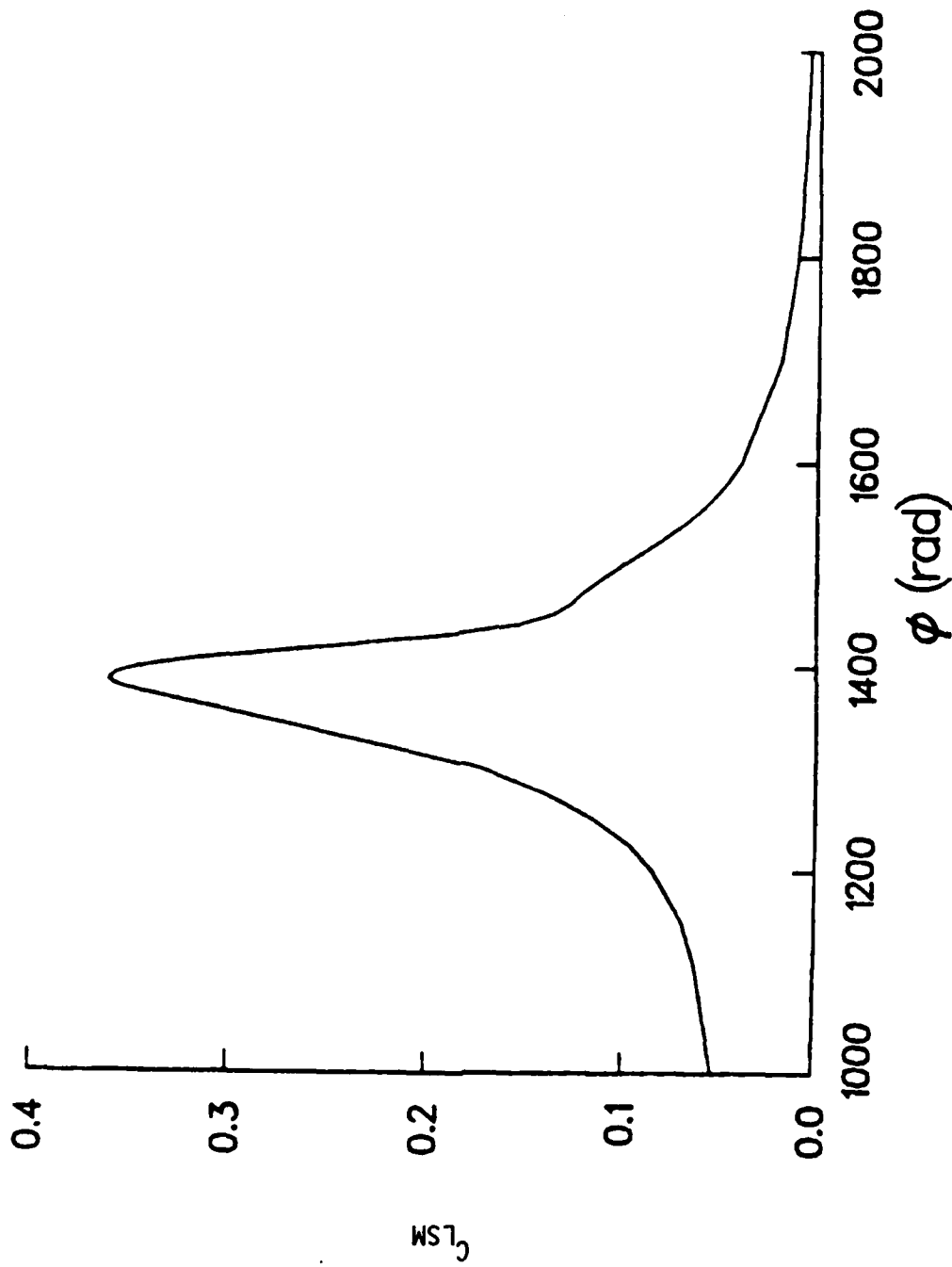


Figure 7. Liquid Side Moment Coefficient C_{LSM} vs Spin Angle for $\tau = .08$ and the Conditions of Figure 5.

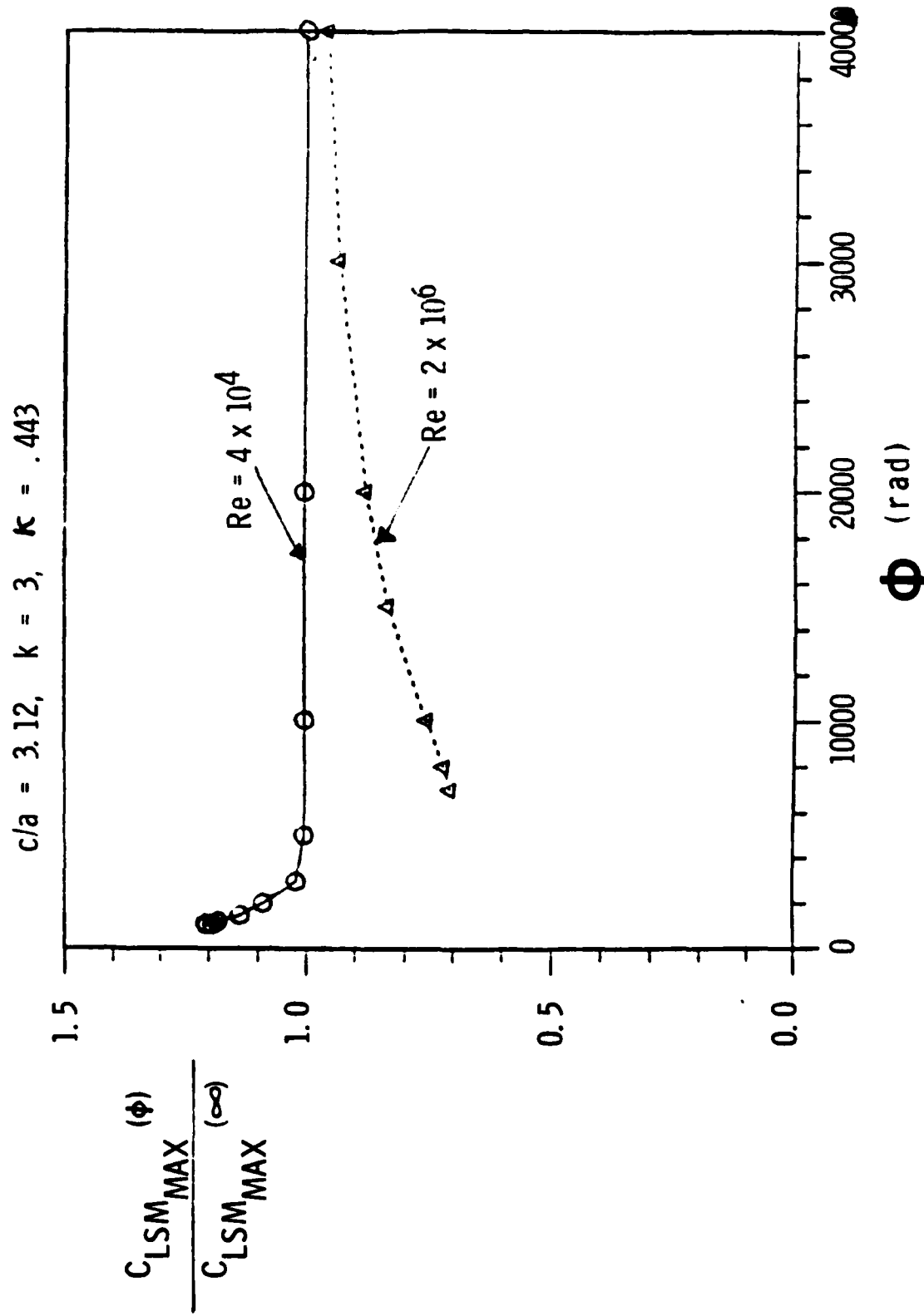


Figure 8. Ratio of Maximum Side Moment Coefficients vs Roll Angle, ϕ for $Re = 4 \times 10^4, 2 \times 10^6, c/a = 3.12, k = 3, n = 1.$

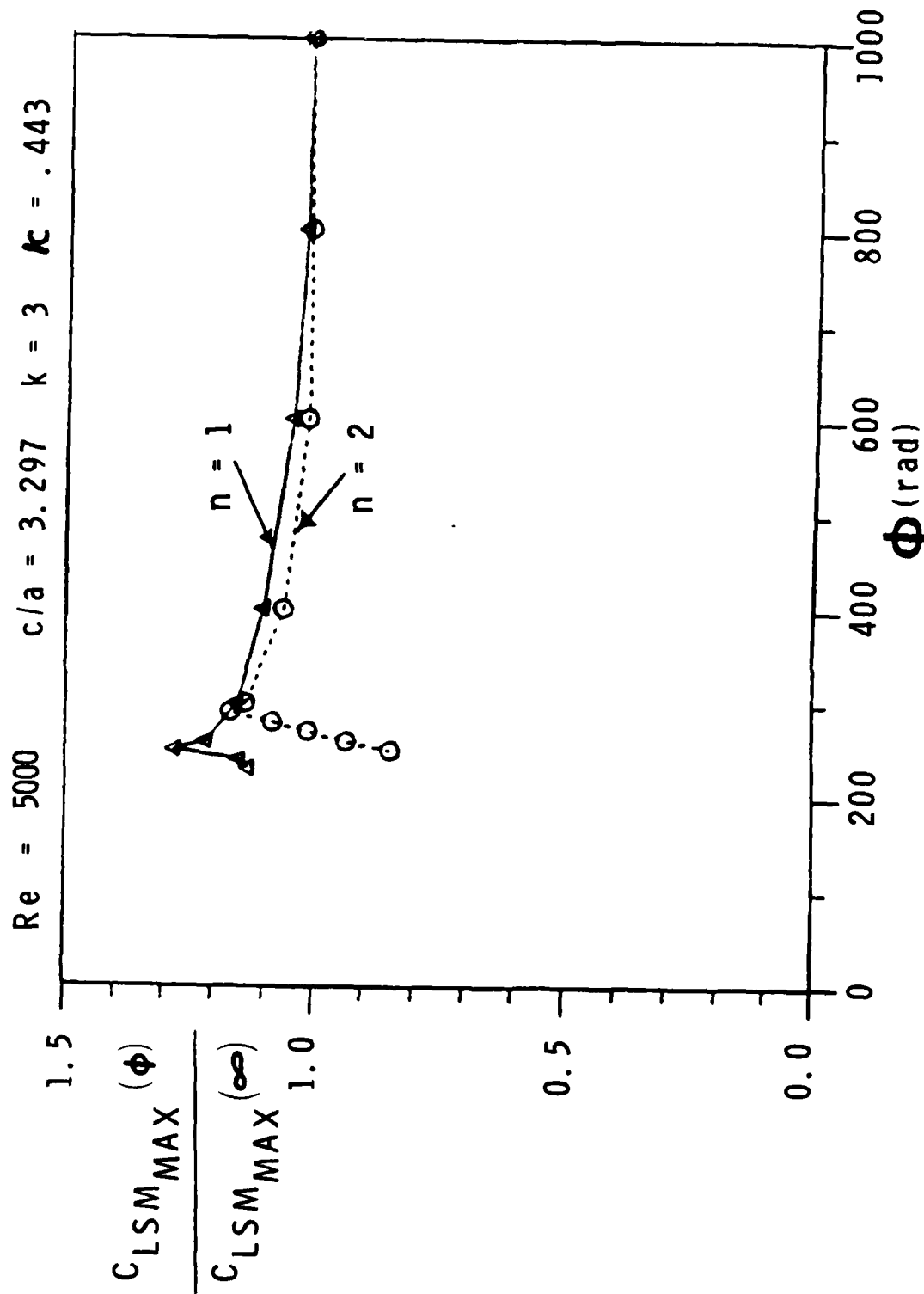


Figure 9. Ratio of Maximum Side Moment Coefficients vs Roll Angle, for $Re = 5000$, $c/a = 3.297$, $k = 3$, $n = 1, 2$.

REFERENCES

1. K. Stewartson, "On the Stability of a Spinning Top Containing Liquid," Journal of Fluid Mechanics, Vol. 5, Part 4, September 1959, pp. 577-592.
2. E.H. Wedemeyer, "Viscous Correction to Stewartson's Stability Criterion," Ballistic Research Laboratory, Aberdeen Proving Ground, Maryland, BRL Report 1325, June 1966. (AD 489687)
3. C.H. Murphy, "Angular Motion of a Spinning Projectile With a Viscous Liquid Payload," Ballistic Research Laboratory, Aberdeen Proving Ground, Maryland, BRL Memorandum Report ARBRL-MR-03194, August 1982. (AD A118676) (See also Journal of Guidance, Control, and Dynamics, Vol. 6, July-August 1983, pp. 280-286.)
4. C.W. Kitchens, Jr., N. Gerber, and R. Sedney, "Oscillations of a Liquid in a Rotating Cylinder: Solid Body Rotation," Ballistic Research Laboratory, Aberdeen Proving Ground, Maryland, BRL Technical Report ARBRL-TR-02081, June 1978. (AD A057759)
5. N. Gerber, R. Sedney, and J.M. Bartos, "Pressure Moment on a Liquid-Filled Projectile: Solid Body Rotation," Ballistic Research Laboratory, Aberdeen Proving Ground, Maryland, BRL Technical Report ARBRL-TR-02422, October 1982. (AD A120567)
6. N. Gerber and R. Sedney, "Moment on a Liquid-Filled Spinning and Nutating Projectile: Solid Body Rotation," Ballistic Research Laboratory, Aberdeen Proving Ground, Maryland, BRL Technical Report ARBRL-TR-02470, February 1983. (AD A125332)
7. C.H. Murphy, "Liquid Payload Roll Moment Induced by a Spinning and Coning Projectile," Ballistic Research Laboratory, Aberdeen Proving Ground, Maryland, BRL Technical Report ARBRL-TR-02521, September 1983. (AD A133681) (See also AIAA Paper 83-2142, August 1983.)
8. A. Mark, "Measurements of Angular Momentum Transfer in Liquid-Filled Projectiles," Ballistic Research Laboratory, Aberdeen Proving Ground, Maryland, BRL Technical Report ARBRL-TR-02029, November 1977. (AD A051056)
9. E.H. Wedemeyer, "The Unsteady Flow Within a Spinning Cylinder," Journal of Fluid Mechanics, Vol. 20, Part 3, 1964, pp. 383-399. (See also BRL Report 1225, October 1963, (AD 431846).)
10. C.W. Kitchens, Jr., "Ekman Compatibility Conditions in Wedemeyer Spin-Up Model," Physics of Fluids, Vol. 23, Part 5, May 1980, pp. 1062-1064.
11. C.W. Kitchens, Jr., N. Gerber, and R. Sedney, "Spin Decay of Liquid-Filled Projectiles," Journal of Spacecraft and Rockets, Vol. 15, November-December 1978, pp. 348-354. (See also BRL Report 1996, July 1977, (AD A043275), and BRL Report 2026, October 1977, (AD A050311).)

REFERENCES (Continued)

12. R. Sedney and N. Gerber, "Viscous Effects in the Wedemeyer Model of Spin-Up From Rest," Ballistic Research Laboratory, Aberdeen Proving Ground, Maryland, BRL Technical Report ARBRL-TR-02493, June 1983. (AD A129506)
13. B.G. Karpov, "Dynamics of Liquid-Filled Shell: Instability During Spin-Up," Ballistic Research Laboratory, Aberdeen Proving Ground, Maryland, BRL Memorandum Report 1629, January 1965. (AD 463926)
14. M.M. Reddi, "On the Eigenvalues of Couette Flow in a Fully-Filled Cylindrical Container," Franklin Institute Research Laboratory, Philadelphia, PA, Report No. F-B2294, 1967.
15. Y.M. Lynn, "Free Oscillations of a Liquid During Spin-Up," Ballistic Research Laboratory, Aberdeen Proving Ground, Maryland, BRL Report No. 1663, August 1973. (AD 769710)
16. R. Sedney and N. Gerber, "Oscillations of a Liquid in a Rotating Cylinder: Part II. Spin-Up," Ballistic Research Laboratory, Aberdeen Proving Ground, Maryland, BRL Technical Report ARBRL-TR-02489, May 1983. (AD A129094)
17. R. Sedney and N. Gerber, "Treatment of the Discontinuity in the Spin-Up Problem with Impulsive Start," Ballistic Research Laboratory, Aberdeen Proving Ground, Maryland, BRL Technical Report ARBRL-TR-02520, September 1983. (AD A133682)

APPENDIX A

VISCOUS COMPONENTS OF SIDE MOMENT

APPENDIX A

The viscous components of the perturbation variables and liquid moment during spin-up differ from the expressions given in Reference 7 in two ways: (1) the boundary condition on w_s as given by Eq. (2.22), and (2) the replacement of Re by $\hat{w}_a Re$ in the end-wall boundary layer profiles.

More specifically, the boundary layer profiles on the lateral wall ($\hat{r} = a$) are:

$$w_{sv} = \left\{ \left[1 + is + a \frac{\partial \hat{w}(a)}{\partial r} \right] (\hat{x}/a) \hat{K} - w_{si}(a, \hat{x}) \right\} e^{(\hat{r}-a)/a\delta_a} \quad (A1)$$

$$u_{sv} = - \left[(i - s) \hat{K} + u_{si}(a, \hat{x}) \right] e^{(\hat{r}-a)/a\delta_a} \quad (A2)$$

The viscous pressure perturbation at the lateral wall is

$$p_{sv}(a, \hat{x}) = 2\delta_a \left\{ \left[1 + is + a \frac{\partial \hat{w}(a)}{\partial r} \right] (\hat{x}/a) \hat{K} - w_{si}(a, \hat{x}) \right\} \quad (A3)$$

On the end walls ($\hat{x} = \pm c$), a single complex velocity profile is required for the viscous liquid moment integral:

$$w_{sv} - i v_{sv} = \mp \left\{ w_{si}(\hat{r}, c) - i v_{si}(\hat{r}, c) - \left[2(1 + is) + \hat{r} \frac{\partial \hat{w}(\hat{r})}{\partial r} \right] (c/a) \hat{K} \right\} e^{-\beta \frac{c \mp \hat{x}}{c}} \quad (A4)$$

$$\beta = i (c/a) \hat{w}_a^{1/2} \delta_a^{-1} \sqrt{(1 - is)/(1 + is)} \quad (A5)$$

The viscous pressure perturbation is zero on the end walls.

The viscous moment integrals are the same as those given in Reference 7.

$$m_{v\ell} = (2 c \hat{K} Re)^{-1} \int_{-c}^c \left[\hat{x} \frac{\partial w_{sv}}{\partial r} + i a \frac{\partial u_{sv}}{\partial r} \right]_{\hat{r} = a} d\hat{x} \quad (A6)$$

$$m_{ve} = (a \hat{K} Re)^{-1} \int_0^a \left[\frac{\partial}{\partial x} (w_{sv} - i v_{sv}) \right]_{\hat{x} = c} \hat{r} d\hat{r} \quad (A7)$$

LIST OF SYMBOLS

A_0	coefficient in the expansion of X_0 ; see Eqs. (2.45) and (4.12-13)
$A_k, A_{en}, A_{\ell k}$	coefficients in the expansions of $X_k, X_{en}, X_{\ell k}$
a	radius of a liquid-filled cylindrical cavity
a_{en}	coefficients in the expansion (4.18) of r/a ; the solution of system (4.19)
$a_{\ell k}$	coefficients in the expansion (4.8) of x/c ; the solution of system (4.9)
B_0	coefficient in the expansion of X_0 ; see Eqs. (2.45) and (4.25)
$B_k, B_{en}, B_{\ell k}$	coefficients in the expansions of $X_k, X_{en}, X_{\ell k}$
b_j	defined by Eq. (4.10)
b_{jk}	defined by Eq. (4.11)
C_{LIM}	liquid in-plane moment coefficient
C_{LSM}	liquid side moment coefficient
c	one-half the length of the liquid-filled cylindrical cavity
c_j	defined by Eq. (4.24)
c_{jn}	defined by Eq. (4.25)
D	$D(r,t)$ defined by Eq. (2.39)
$d_{en}, d_{\ell k}$	defined by Eq. (4.1)

LIST OF SYMBOLS (Continued)

I	liquid angular momentum ratio, Eq. (2.7)
J_m	Bessel function of the first kind of order m
\hat{K}	$K_{10} \exp(i \phi_{10})$
K_{10}	magnitude of the coning motion
k_ℓ	$\kappa (a/c) \text{Re}^{-1/2}$
k_t	$.035 (a/c) \text{Re}^{-1/5}$
m	azimuthal wave number in Eqs. (2.8 - 2.11); $m = 0, \pm 1, \pm 2, \dots$
\hat{m}	$ m $
$m_{pe}, m_{p\ell}$	non-dimensional liquid moment due to end-wall and lateral pressure, respectively
$m_{ve}, m_{v\ell}$	non-dimensional liquid moment due to end-wall and lateral viscous force, respectively
N_e, N_ℓ	maximum values of k and n , respectively, considered in the end-wall and lateral expansions, Eq. (4.1)
p	liquid pressure
p_0, p_e, p_ℓ	components of p_{sj} , Eq. (4.1)
p_s	liquid pressure perturbation
p_{sj}, p_{sv}	inviscid and viscous components of p_s

LIST OF SYMBOLS (Continued)

\hat{p}	defined by Eq. (2.12)
r, \hat{r}	radial coordinates in the inertial and aeroballistic systems, respectively
r_f	the front: the r value separating the rotating and non-rotating fluid
Re	$a^2 \phi / \nu$, Reynolds number
$R_{en}, R_{\ell k}$	functions of r in the expansion of p_{sj} , Eq. (4.1)
$R_{env}, R_{\ell kv}$	defined by Eq. (4.3)
$R_{enw}, R_{\ell kw}$	defined by Eq. (4.4)
R_k	function of r in the expansion for p_{sj} , Eq. (2.41)
R_{kv}	defined by Eq. (3.3)
s	$(\epsilon + i) \tau$
s_{kn}	eigenvalue of s : a value of s that satisfies Eq. (3.2)
t	time
u_s, v_s, w_s	components of the liquid velocity perturbation in the inertial system
u_{si}, v_{si}, w_{si}	inviscid part of u_s, v_s, w_s
u_{sv}, v_{sv}, w_{sv}	viscous part of u_s, v_s, w_s

LIST OF SYMBOLS (Continued)

V_x, V_r, V_θ	velocity components of the liquid in the inertial cylindrical system
\hat{w}	$V_\theta (r\dot{\phi})^{-1}$ for $\hat{K} = 0$
\hat{w}_a	average value of \hat{w} , Eqs. (2.34 - 2.35)
x, \hat{x}	axial coordinates in the inertial and aeroballistic systems, respectively
χ_{en}, χ_{ek}	functions of x in the expansion of p_{sj} , Eq. (4.1)
χ_k	function of x in the expansion of p_{sj} , Eq. (2.41)
$\hat{\alpha}, \hat{\beta}$	angles of attack and side-slip, respectively, in the aeroballistic system
δ_a, δ_c	functions of $(c/a, Re, m, s)$, defined by Eqs. (2.32 - 2.33)
ϵ	exponential damping per cycle of coning motion
κ	parameter in k_ℓ , usually 0.5
$\theta, \hat{\theta}$	azimuthal coordinates in the inertial and aeroballistic systems, respectively
λ_k	a constant in Eqs. (2.42) and (2.46)
$\hat{\lambda}_k$	$[-D/(s - m \hat{w} i)^2]^{1/2} \lambda_k$
$\lambda_{en}, \lambda_{ek}$	constants in the expressions for χ_{en}, χ_{ek} , respectively
ν	kinematic viscosity

LIST OF SYMBOLS (Continued)

ρ_L	liquid density
τ	ratio of coning frequency to spin frequency
τ_{kn}	eigenvalue of τ
ϕ	$\dot{\phi}t$, spin angle
ϕ_{10}	orientation angle of \hat{K}
$\dot{\phi}$	spin rate

DISTRIBUTION LIST

<u>No. of Copies</u>	<u>Organization</u>	<u>No. of Copies</u>	<u>Organization</u>
12	Administrator Defense Technical Information Center ATTN: DTIC-DDA Cameron Station Alexandria, VA 22314	1	Commander US Army Armament Munitions and Chemical Command ATTN: DRSMC-LEP-L(R) Rock Island, IL 61299
1	Commander US Army Engineer Waterways Experiment Station ATTN: R.H. Malter P. O. Box 631 Vicksburg, MS 39180	1	Director Benet Weapons Laboratory Armament R&D Center US Army AMCCOM ATTN: DRSMC-LCB-TL(D) Watervliet, NY 12189
1	Commander US Army Materiel Development and Readiness Command ATTN: DRCDMD-ST 5001 Eisenhower Avenue Alexandria, VA 22333	1	Commander US Army Aviation Research and Development Command ATTN: DRDAV-E 4300 Goodfellow Blvd St. Louis, MO 63120
1	Commander Armament R&D Center US Army AMCCOM ATTN: DRSMC-TDC(D) Dover, NJ 07801	1	Director US Army Air Mobility Research and Development Laboratory ATTN: SAVDL-D, W.J. McCroskey Ames Research Center Moffett Field, CA 94035
3	Commander Armament R&D Center US Army AMCCOM ATTN: DRSMC-TSS(D) Dover, NJ 07801	1	Commander US Army Communications Research and Development Command ATTN: DRSEL-ATDD Fort Monmouth, NJ 07703
6	Commander Armament R&D Center US Army AMCCOM ATTN: DRSMC-LCA-F(D) Mr. D. Mertz Mr. E. Falkowski Mr. A. Loeb Mr. R. Kline Mr. S. Kahn Mr. S. Wasserman Dover, NJ 07801	1	Commander US Army Communications and Development Command ATTN: DRSEL-L Fort Monmouth, NJ 07703
1	Commander US Army Communications Rsch and Development Command ATTN: DRSEL-ATDD Fort Monmouth, NJ 07703	1	Commander US Army Electronics Research and Development Command Technical Support Activity ATTN: DELSD-L Fort Monmouth, NJ 07703
		1	HQDA DAMA-ART-M Washington, DC 20310

DISTRIBUTION LIST

<u>No. of Copies</u>	<u>Organization</u>	<u>No. of Copies</u>	<u>Organization</u>
1	Commander US Army Missile Command ATTN: DRSMI-YDL Redstone Arsenal, AL 35898	2	Commandant US Army Infantry School ATTN: ATSH-CD-CSO-OR Fort Benning, GA 31905
1	Commander US Army Missile Command ATTN: DRSMI-R Redstone Arsenal, AL 35898	3	Commander Naval Air Systems Command ATTN: AIR-604 Washington, DC 20360
1	Commander US Army Missile Command ATTN: DRSMI-RDK, Mr. R. Deep Redstone Arsenal, AL 35898	2	Commander David W. Taylor Naval Ship Research & Development Cmd ATTN: H.J. Lugt, Code 1802 S. de los Santos Bethesda, MD 20084
1	Commander US Army Tank Automotive Research & Development Command ATTN: DRSTA-TSL Warren, MI 48090	1	Commander Naval Surface Weapons Center ATTN: DX-21, Lib Br Dahlgren, VA 22448
1	Director US Army TRADOC Systems Analysis Activity ATTN: ATAA-SL White Sands Missile Range, NM 88002	4	Commander Naval Surface Weapons Center Applied Aerodynamics Division ATTN: J.T. Frasier M. Ciment A.E. Winklemann W.C. Ragsdale Silver Spring, MD 20910
1	Commander US Army Jefferson Proving GD ATTN: STEJP-TD-D Madison, IN 47251	1	AFATL (DLDL, Dr. D.C. Daniel) Eglin AFB, FL 32542
2	Commander US Army Research Office ATTN: Dr. R.E. Singleton Dr. Jagdish Chandra P.O. Box 12211 Research Triangle Park, NC 27709	2	AFWAL (W.L. Hankey; J.S. Shang) Wright-Patterson AFB, OH 45433
1	AGARD-NATO ATTN: R.H. Korkegi APO New York 09777	1	Aerospace Corporation Aero-Engineering Subdivision ATTN: Walter F. Reddall El Segundo, CA 90245
1	AFWL/SUL Kirtland AFB, NM 87117	1	Commander US Army Development & Employment Agency ATTN: MODE-TED-SAB Fort Lewis, WA 98433

DISTRIBUTION LIST

<u>No. of Copies</u>	<u>Organization</u>	<u>No. of Copies</u>	<u>Organization</u>
5	Director National Aeronautics and Space Administration Ames Research Center ATTN: D.R. Chapman J. Rakich W.C. Rose B. Wick P. Kutler Moffett Field, CA 94035	2	Director Jet Propulsion Laboratory ATTN: L.M. Mach Tech Library 4800 Oak Grove Drive Pasadena, CA 91109
4	Director National Aeronautics and Space Administration Langley Research Center ATTN: E. Price J. South J.R. Sterrett Tech Library Langley Station Hampton, VA 23365	3	Arnold Research Org., Inc. ATTN: J.D. Whitfield R.K. Matthews J.C. Adams Arnold AFB, TN 37389
1	Director National Aeronautics and Space Administration Lewis Research Center ATTN: MS 60-3, Tech Lib 21000 Brookpark Road Cleveland, OH 44135	1	AVCO Systems Division ATTN: B. Reeves 201 Lowell Street Wilmington, MA 01887
2	Director National Aeronautics and Space Administration Marshall Space Flight Center ATTN: A.R. Felix, Chief S&E-AERO-AE Dr. W.W. Fowles Huntsville, AL 35812	3	Boeing Commercial Airplane Company ATTN: R.A. Day, MS 1W-82 P.E. Rubbert, MS 3N-19 J.D. McLean, MS-3N-19 Seattle, WA 98124
3	Aerospace Corporation ATTN: H. Mirels R.L. Varwig Aerophysics Lab. P.O. Box 92957 Los Angeles, CA 90009	3	Calspan Corporation ATTN: A. Ritter G. Homicz W. Rae P.O. Box 400 Buffalo, NY 14225
		1	General Dynamics ATTN: Research Lib 2246 P.O. Box 748 Fort Worth, TX 76101
		1	General Electric Company, RESD ATTN: W.J. East 3198 Chestnut Street Philadelphia, PA 19101
		2	Grumman Aerospace Corporation ATTN: R.E. Melnik L.G. Kaufman Bethpage, NY 11714

DISTRIBUTION LIST

<u>No. of Copies</u>	<u>Organization</u>	<u>No. of Copies</u>	<u>Organization</u>
2	Lockheed-Georgia Company ATTN: B.H. Little, Jr. G.A. Pounds Dept 72074, Zone 403 86 South Cobb Drive Marietta, GA 30063	2	United Aircraft Corporation Research Laboratory ATTN: M.J. Werle Library East Hartford, CT 06108
1	Lockheed Missiles and Space Company ATTN: Tech Info Center 3251 Hanover Street Palo Alto, CA 94304	1	Vought Corporation ATTN: J.M. Cooksey, Chief, Gas Dynamics Lab, 2-53700 P.O. Box 5907 Dallas, TX 75222
3	Martin-Marietta Corporation ATTN: S.H. Maslen S.C. Traugott H. Obremski 1450 S. Rolling Road Baltimore, MD 21227	1	Arizona State University Department of Mechanical and Energy Systems Engineering ATTN: G.P. Neitzel Tempe, AZ 85281
2	McDonnell Douglas Astronautics Corporation ATTN: J. Xerikos H. Tang 5301 Bolsa Avenue Huntington Beach, CA 92647	1	Cornell University Graduate School of Aero Engr ATTN: Library Ithaca, NY 14850
1	Douglas Aircraft Company ATTN: T. Cebeci 3855 Lakewood Boulevard Long Beach, CA 90846	3	California Institute of Technology ATTN: Tech Library H.B. Keller, Math Dept D. Coles, Aero Dept Pasadena, CA 91109
3	Rockwell International Science Center ATTN: Dr. V. Shankar Dr. N. Malmuth Dr. S. Chakravarthy 1049 Camino Dos Rios Thousand Oaks, CA 91360	1	Illinois Institute of Tech ATTN: H. M. Nagib 3300 South Federal Chicago, IL 60616
4	Director Sandia National Laboratory ATTN: F.G. Blottner W.L. Oberkampf H.W. Vaughn Technical Lib. Albuquerque, NM 87115	1	The Johns Hopkins University Dept of Mech and Materials Sci. ATTN: S. Corrsin Baltimore, MD 21218
		1	Louisiana State University Dept. of Physics and Astronomy ATTN: Dr. R.G. Hussey Baton Rouge, LA 70803

DISTRIBUTION LIST

<u>No. of Copies</u>	<u>Organization</u>	<u>No. of Copies</u>	<u>Organization</u>
4	Director Johns Hopkins University Applied Physics Laboratory ATTN: Dr. R.D. Whiting Dr. D.A. Hurdif Dr. R.S. Hirsh Mr. E.R. Bohn Johns Hopkins Road Laurel, MD 20707	2	Polytechnic Institute of New York ATTN: G. Moretti S.G. Rubin Route 110 Farmingdale, NY 11735
3	Massachusetts Institute of Technology ATTN: E. Covert H. Greenspan Tech Lib 77 Massachusetts Avenue Cambridge, MA 02139	3	Princeton University James Forrestal Research Ctr Gas Dynamics Laboratory ATTN: S.M. Bogdonoff S.I. Cheng Tech Library Princeton, NJ 08540
2	North Carolina State Univ Mechanical and Aerospace Engineering Department ATTN: F.F. DeJarnette J.C. Williams Raleigh, NC 27607	1	Purdue University Thermal Science & Prop Ctr ATTN: Tech Library W. Lafayette, IN 47906
1	Northwestern University Department of Engineering Science and Applied Mathematics ATTN: Dr. S.H. Davis Evanston, IL 60201	1	Rensselaer Polytechnic Institute Department of Math Sciences ATTN: R.C. Diprima Troy, NY 12181
1	Notre Dame University Department of Aero Engr ATTN: T.J. Mueller South Bend, IN 46556	1	Rutgers University Department of Mechanical, Industrial, and Aerospace Engineering ATTN: R.H. Page New Brunswick, NJ 08903
2	Ohio State University Dept of Aeronautical and Astronautical Engineering ATTN: S.L. Petrie O.R. Burggraf Columbus, OH 43210	1	San Diego State University Department of Aerospace Engr and Engineering Mechanics College of Engineering ATTN: K.C. Wang San Diego, CA 92182
		1	Southern Methodist University Department of Civil and Mechanical Engineering ATTN: R.L. Simpson Dallas, TX 75222

DISTRIBUTION LIST

<u>No. of Copies</u>	<u>Organization</u>	<u>No. of Copies</u>	<u>Organization</u>
1	Southwest Research Institute Applied Mechanics Reviews 8500 Culebra Road San Antonio, TX 78228	2	University of Maryland ATTN: W. Melnik J.D. Anderson College Park, MD 20740
2	Stanford University Dept of Aeronautics/Astronautics ATTN: Dr. J.L. Steger Dr. S. Chakravarthy Stanford, CA 94305	1	University of Maryland - Baltimore County Department of Mathematics ATTN: Dr. Y.M. Lynn 5401 Wilkens Avenue Baltimore, MD 21228
1	Texas A&M University College of Engineering ATTN: R.H. Page College Station, TX 77843	1	University of Santa Clara Department of Physics ATTN: R. Greeley Santa Clara, CA 95053
1	University of California - Davis ATTN: H.A. Dwyer Davis, CA 95616	2	University of Southern California Department of Aerospace Engineering ATTN: T. Maxworthy P. Weidman Los Angeles, CA 90007
1	University of California - Berkeley Department of Aerospace Engineering ATTN: M. Holt Berkeley, CA 94720	2	University of Michigan Department of Aeronautical Engineering ATTN: W.W. Wilmarth Tech Library East Engineering Building Ann Arbor, MI 48104
2	University of California - San Diego Department of Aerospace Engineering and Mechanical Engineering Sciences ATTN: P. Libby Tech Library La Jolla, CA 92037	2	University of Rochester Department of Mechanical and Aerospace Sciences ATTN: R. Gans A. Clark, Jr. Rochester, NY 14627
1	University of Cincinnati Department of Aerospace Engineering ATTN: R.T. Davis Cincinnati, OH 45221	1	University of Tennessee Department of Physics ATTN: Prof. W.E. Scott Knoxville, TN 37916
1	University of Colorado Department of Astro-Geophysics ATTN: E.R. Benton Boulder, CO 80302		

DISTRIBUTION LIST

<u>No. of Copies</u>	<u>Organization</u>	<u>No. of Copies</u>	<u>Organization</u>
1	University of Texas Department of Aerospace Engineering ATTN: J.C. Westkaemper Austin, TX 78712	1	Woods Hole Oceanographic Institute ATTN: J.A. Whitehead Woods Hole, MA 02543
1	University of Virginia Department of Aerospace Engineering & Engineering Physics ATTN: I.D. Jacobson Charlottesville, VA 22901	3	Virginia Polytechnic Institute and State University Department of Aerospace Engineering ATTN: Tech Library Dr. W. Saric Dr. T. Herbert Blacksburg, VA 24061
1	University of Virginia Research Laboratories for the Engineering Sciences ATTN: Prof. H. G. Wood P.O. Box 3366 University Station Charlottesville, VA 22901		<u>Aberdeen Proving Ground</u> Director, USAMSAA ATTN: DRXSY-D DRXSY-MP, H. Cohen
1	University of Washington Department of Mechanical Engineering ATTN: Tech Library Seattle, WA 98105		Commander, USATECOM ATTN: DRSTE-TO-F
1	University of Wyoming ATTN: D.L. Boyer University Station Laramie, WY 82071		Cdr, CRDC, AMCCOM ATTN: DRSMC-CLN(A) W. C. Dee DRSMC-CLB-PA(A) M. C. Miller DRSMC-CLJ-L(A)
1	U.S. Military Academy Department of Physics ATTN: MAJ G. Heuser West Point, NY 10996		

USER EVALUATION SHEET/CHANGE OF ADDRESS

This Laboratory undertakes a continuing effort to improve the quality of the reports it publishes. Your comments/answers to the items/questions below will aid us in our efforts.

1. BRL Report Number _____ Date of Report _____

2. Date Report Received _____

3. Does this report satisfy a need? (Comment on purpose, related project, or other area of interest for which the report will be used.) _____

4. How specifically, is the report being used? (Information source, design data, procedure, source of ideas, etc.) _____

5. Has the information in this report led to any quantitative savings as far as man-hours or dollars saved, operating costs avoided or efficiencies achieved, etc? If so, please elaborate. _____

6. General Comments. What do you think should be changed to improve future reports? (Indicate changes to organization, technical content, format, etc.) _____

CURRENT
ADDRESS

Name

Organization

Address

City, State, Zip

7. If indicating a Change of Address or Address Correction, please provide the New or Correct Address in Block 6 above and the Old or Incorrect address below.

OLD
ADDRESS

Name

Organization

Address

City, State, Zip

(Remove this sheet along the perforation, fold as indicated, staple or tape closed, and mail.)

FOLD HERE

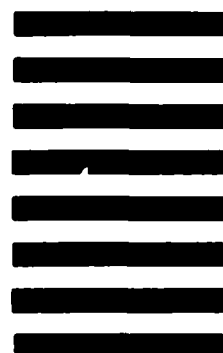
Director
JS Army Ballistic Research Laboratory
ATTN: DRXBR-OD-ST
Aberdeen Proving Ground, MD 21005-5066



NO POSTAGE
NECESSARY
IF MAILED
IN THE
UNITED STATES

OFFICIAL BUSINESS
PENALTY FOR PRIVATE USE, \$300

BUSINESS REPLY MAIL
FIRST CLASS PERMIT NO 12062 WASHINGTON, DC
POSTAGE WILL BE PAID BY DEPARTMENT OF THE ARMY



Director
US Army Ballistic Research Laboratory
ATTN: DRXBR-OD-ST
Aberdeen Proving Ground, MD 21005-9989

FOLD HERE